Environmental Earth Sciences (2024) 83:110
https://doi.org/10.1007/s12665-023-11374-4

ORIGINAL ARTICLE

Slope stability analysis applied to the 5th section of the Northern Marmara Motorway, İzmit, Türkiye

Müge Çakıner[1] · Erkan Bozkurtoğlu[2] · Ahmet Karakaş[3]

Received: 11 November 2022 / Accepted: 12 December 2023 / Published online: 29 January 2024

Abstract
The Northern Marmara Motorway is a project that aims to alleviate the heavy traffic congestion in the provinces of İstanbul, Tekirdağ, Kocaeli and Adapazarı. Within the 5th section bounded by "the Motorway Port Connection Road" and "İzmit Intersection", mass movements of slide (Y1, Y2) and flow (Y3) types were observed along the route. This study investigated the causes of mass movements in the Korucu Formation, which consists of sandstone and shale alternation. It also evaluated the support systems to prevent these movements. The analysis considered project criteria, both static and dynamic conditions, types of mass movements and triggering factors. The study identified a combination of factors, including the water table and surface waters, which lead to progressive weathering and mass movement. Stability analyses were conducted for specific right-cut slope sections. These analyses included assessments of soil structure, soil–rock mechanics, engineering geology and geotechnics, as well as examination of field and laboratory test results. These analyses aimed to comprehensively investigate and understand the factors influencing the occurrence of mass movements, particularly for km: 170 + 300–170 + 400, km: 170 + 640 and km: 175 + 297–175 + 463. At Y1, pile retaining walls are proposed using Slide2 software to reduce the slope angle from 22° to 17°. At Y2, a translational landslide occurred with recommendations for the adjustment of the slope angle and protective measures considering the disturbance factors ($D = 0.3$ and $D = 0.5$). Y3 was a flow-type movement that required protection of the slope with riprap due to the different geological conditions and disturbance factors. This study underlines the need for a comprehensive geological analysis and structural measures to ensure safety in these areas.

Keywords Slope stability · Motorway · Geological engineering · Remedial measures · Geology

Introduction

The growing populations and developing economies of countries around the world require a rapid flow of transportation between cities and countries. There is a need for highways that run outside settlements, have few curves, do not intersect with other roads, are separated in the middle in two directions, and have three or more lanes in each direction. One of the roads built for this purpose in the Marmara region of Turkiye is the North Marmara highway. The Kurtköy–Akyazı section (including the connecting roads) of the Northern Marmara Motorway (including the 3rd Bosphorus Bridge) was built with the Build–Operate–Transfer (BOT) model between the Port Connection Road and the Izmit Intersection. The 5th section starts at km: 151 + 500 just after the port intersection on the main motorway and ends at the exit of the T-4 tunnel at km: 188 + 184.61. There are also two intersections on this stretch: the Sevindikli intersection at km: 168 + 224 and the Toylar intersection at km:175 + 707 (Fig. 1). This study aims to evaluate the causes of mass movements and the applications for embankment support applied on the Kurtköy–Akyazı (5th Section) of the Northern Marmara Motorway (including the 3rd

✉ Müge Çakıner
cakiner@itu.edu.tr

Erkan Bozkurtoğlu
erkan@itu.edu.tr

Ahmet Karakaş
akarakas@kocaeli.edu.tr

1 Graduate School, Istanbul Technical University (İTÜ), Maslak, TR−34469 Istanbul, Turkey

2 Faculty of Mines, Department of Geological Engineering, Istanbul Technical University (İTÜ), Maslak, TR−34469 Istanbul, Turkey

3 Engineering Faculty, Geological Engineering Department, Kocaeli University, İzmit 41001, Kocaeli, Turkey

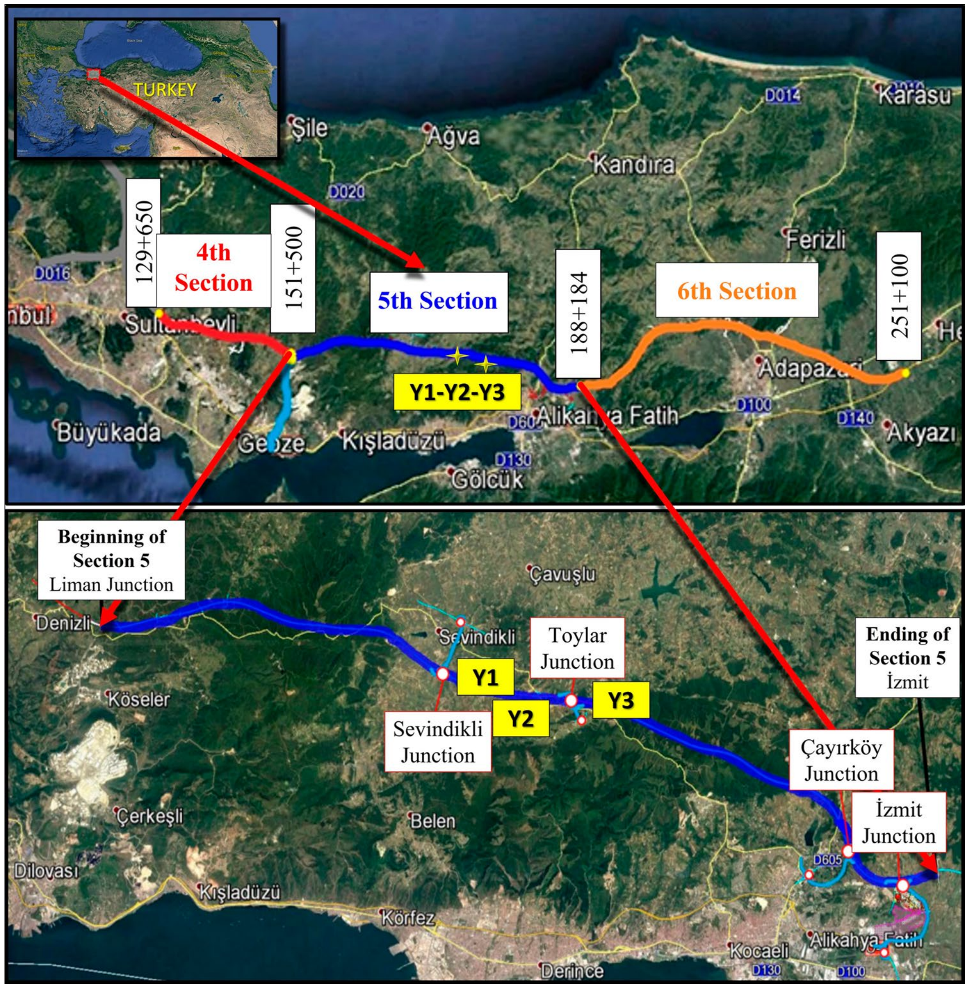

Fig. 1 Satellite image showing the 5th Section of the Northern Marmara Motorway (Google Earth 2020)

Bosphorus Bridge) Project (between Port Connection Road-İzmit Intersection).

Earlier studies conducted in the Kocaeli region provided information about mass movements and references to the study. Karakaş and Coruk (2011) investigated the causes and effects of mass movements that occurred in the tectonic units in the south and north of Kocaeli province. Arslan et al. (2014, 2015, 2016, 2022) conducted a study aimed at minimizing the risk of landslides by establishing a fiber optic monitoring system in the Bahçecik region of Kocaeli. Ulamış et al. (2017) investigated the estimation of seismic slope displacements in the North Anatolian Fault Zone, Kocaeli Karamürsel area. The study conducted by Güven (2022) on Derince City, which refers to the seismic vulnerability index and correlates with the 1999 Kocaeli earthquake, provides important insights for analyzing slope stability in seismic areas. Zengince and Karakaş (2018) studied the causes and effects of landslides in the Kocaeli Gölcük area and the remediation measures taken. Kaçka (2019) conducted a study on seismic deformation analysis of landslides in the south and southwest of Karamursel (Kocaeli) district. Yağızel and Özyavaş (2020) investigated the relationship between the mass movements that occur in the south of Izmit Bay and the fracture systems. Similar earlier studies in different parts of the world also provided important insights into mass movements. First, various classifications of mass movements have been made and used by different researchers (Sharpe 1938; Terzaghi 1950; Varnes 1950; 1958; 1978; Baker 1958; Eckel 1958; Bates and Jackson 1987; Hutchinson 1988; EPOCH 1993; Evans and Hungr 1993; Erguvanlı 1995; Suárez 1998; Aleotti and Chowdhury 1999; Ayala 2000; Vallejo et al. 2002; Tarhan 2002; Ertunç 2003; Güney 2004; USGS 2004; Ünsal 2006; Akkuş 1995; 2007; Ayala et al. 2008; Erinç 2010; Hungr et al. 2013). Varnes (1978) classified the types of mass movement according to the type of movement and the properties of the material. Shroder and Bishop (1998) studied mass movements in the Himalayas. Chen and Lee (2004) investigated geohazards of slope mass movements in Hong Kong and the prevention of potential geohazards. Claessens et al. (2013) presented a study on how different variances in slope inclination trigger mass movements. Tiranti et al. (2016) investigated the causes of torrential mass movements that occurred in the Western Alps. Micu et al. (2016) conducted a comprehensive study on mass movements in Romania, one of the areas in Europe where landslides occur most frequently. The effects of landslides on local infrastructure and the environment were investigated by Skrzypczak et al. (2017) for the Polish Sub-Carpathian Voivodeship region in Polish province of Sub-Carpathian. Guerra et al. (2017) conducted a study covering both Brazil and the United Kingdom, looking at slope processes related to mass movement and soil erosion and the factors contributing to the current process along with physical and human influences. Tang et al. (2018) investigated the change in the volume of loose material due to postseismic and coseismic landslides in and around the cities of Yingxiu and Longchi, China. Zhou et al. (2020) investigated the causes of the Shuicheng landslide that occurred in 2019 and analyzed the quantitative mass movement. Sadigov (2020) ran a simulation study to track mass movement during landslide processes in an agricultural landscape. Chiarle et al. (2021) conducted a study to investigate the relationship between mass movements and climate change in the Canadian Cordillera and the European Alps. Muchlis et al. (2021) carried out a study to mitigate the destruction caused by mass movements and reduce the impact of the threat in the Wonolelo area and its surroundings, the Bantul Regency-Yogyakarta Special Region. Babichev et al. (2021) conducted a risk analysis study for a slope mass movement in the Verhnie Vodiane and Solotvyno region, Ukraine.

This study investigated the factors contributing to the occurrence of three mass movements (Y1, Y2 and Y3) in the 5th section of the Northern Marmara Motorway specifically along the road cuts from km: 170 + 300 to km: 175 + 463. Field investigations and engineering geology studies were carried out as part of the study. In addition, the physical and the mechanical properties of the geological units were determined by drilling, field, and laboratory investigations. A slope stability analysis was performed by the Rocscience Slide2 (2004) software using the limit equilibrium methods of Bishop (1955), Janbu (1957, 1973) and Spencer (1967) for the three mass movements (Y1, Y2, and Y3). The analysis results were evaluated to develop slope support systems. Finally, some remedial measures were proposed to improve the slope stability of the three mass movements (Y1, Y2, and Y3).

It is crucial to emphasize distinctive contributions and novelty of this study within the existing scientific literature. While previous studies have provided valuable insights into mass movements globally, this study, the proposed solutions and precautions implemented in the project focus specifically on the Kurtköy–Akyazı Sect. (5th section) of the Northern Marmara Motorway, setting it apart from the broader body of literature. This region presents unique geological and topographical challenges, compounded by the intricate engineering considerations of the highway infrastructure. This study examines the causes of three specific mass movements (Y1, Y2, and Y3) along the road-cut slopes. What distinguishes this study is the comprehensive approach, integrating field and engineering geology studies. By merging detailed geological data, laboratory tests, and cutting-edge analysis methods, this study offers a localized and site-specific solution contributing to the broader field. This approach facilitates the formulation of tailored mitigation measures and slope support systems to enhance the stability of the studied mass movements. The significance of this study lies not only in its direct applicability to the Northern Marmara Motorway but also in its potential to inform similar infrastructure projects worldwide grappling with comparable geological challenges, thereby advancing knowledge in the field of slope stability and mass movement mitigation.

Study area

The study area is located in the middle section of the Northern Marmara Motorway. The project route within Kocaeli Province is referred to as the 5th section, which starts at Liman Junction (km: 151 + 500.00) and ends at Sevindikli Junction (km: 168 + 224.00), Toylar Junction (km: 175 + 707.00) and then connects to the 6th section of the Northern Marmara Motorway at km: 188 + 184.61, as shown in Fig. 1. Consequently, the 5th section is approximately 37 km long.

The mass movements that occurred throughout the study area were designated Y1, Y2, and Y3 (Fig. 1). The mass movement that occurred between km: 170 + 300–170 + 400 was designated Y1, the one that occurred between km: 170 + 640 was designated Y2 and finally the mass movement that occurred between km: 175 + 297–175 + 463 was designated Y3. The type of mass movement Y1 was defined as rotational landslide, the type of mass movement Y2 was defined as translational landslide, and the type of mass movement Y3 was defined as flow. Stability assessments were carried out for each mass movement as part of the study. Table 1 shows summarized information on the kilometers, cut heights, and inclinations of the slopes along the 5th section.

Table 1 Summary table containing the kilometers, cut heights and gradient of slopes of the regions where slope deteriorations occur and their properties

No	Km		Axis	Cut heights (m)	Gradient of slopes (H: V)
Y1	170 + 300	170 + 400	Right	32	2.5:1 & 3:1
Y2	170 + 640		Right	40	2.5:1 & 3:1
Y3	175 + 297	175 + 463	Right	27	3:1

Geological setting

The province of Kocaeli is an important settlement area located on the Kocaeli peninsula in the north and the Armutlu peninsula in the south. The Kocaeli region is represented by lithologic units belonging to two different tectonic units located in the north and south of the North Anatolian Fault Zone (Karakaş and Coruk 2011). The study area is located on the northern tectonic unit. The cut areas where mass movements occurred are located in the Ypresian Korucu Formation, which consists of claystone, siltstone, sandstone, marl and shale (Timur 2002; Altınlı 1968) (Fig. 2). The borehole logs showed a dense mainly claystone–siltstone lithology. The units observed on site show high weathering, soil deposition, and fragmentation in the upper layers, while the lower layers show moderate weathering, less fragmentation, and weak strength. As the claystone is impermeable, it impedes groundwater permeability. In highly fractured units, however, water seeps through claystone fractures and saturates the underlying permeable sandy unit. The region where mass movements occur is within agricultural areas where irrigation saturates the recharge environment on the slope by infiltration through the unit. The Korucu Formation (Tek) generally consists of greenish–grayish–yellowish–gray, thin–medium, locally thick-bedded sandstone and greenish–greenish–gray, thin-bedded shale in the terrain. Thick-bedded sandstones can be found in the lower layers of the formation (Fig. 3). The middle and upper parts of the formation are thin–medium-bedded. While the sandstone–shale intercalation is less common, the shale–marl intercalation is dominant in some places where these sections include turbidite features. It rarely contains lenticular conglomerates (Tokay 1954).

Natural hazard evaluation in the 5th section area

The entire 5th section route in the project area is within the first-degree earthquake zone according to the Turkiye Earthquake Hazard Map published by the Ministry of Interior, Disaster and Emergency Management, Earthquake Department (AFAD 2019). Active faults of the region were defined using GeoScience MapViewer (Department of Scientific Documentation and Publicity, 2016) (Fig. 4).

Factor of safety (FS) standards for cut slopes are specified by the Disaster Regulations for Motorway Engineering Structures. The static factor of safety for long-term analyses of slope stability has been considered as greater than or equal to 1.50; on the other hand, the pseudo-static factor of safety (FSPS) for earthquake analyses has been taken as greater than or equal to 1.10 (Ministry of Public Works and Settlement 2006). It is stated that the target factor of safety is 1.10 in equivalent static analyses in the Turkish Earthquake Regulation (TER 2018). Dynamic condition analyses in the study area were made by considering this situation.

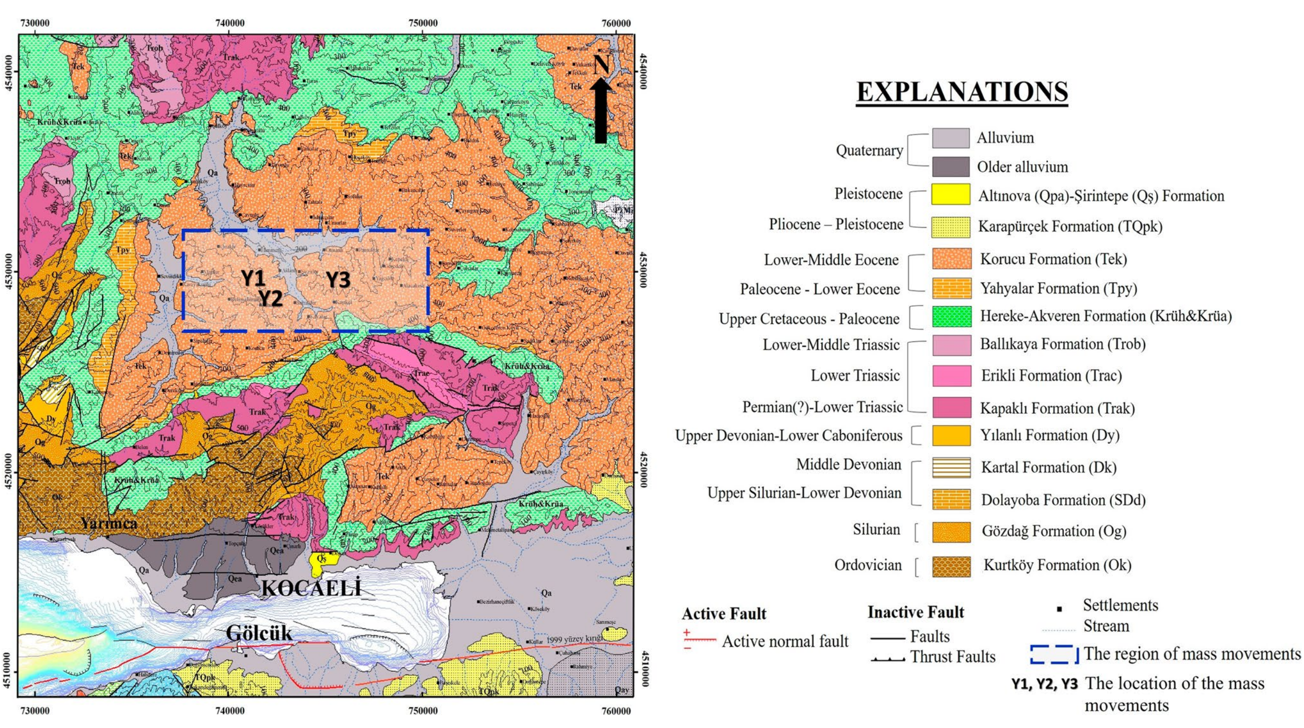

Fig. 2 Geological map of the study area and its surroundings, modified from Tarı (2007)

Fig. 3 A view from the outcrop of the Korucu Formation (Tek) consisting of thin–medium thick-bedded sandstone, and thin-bedded shale alternation

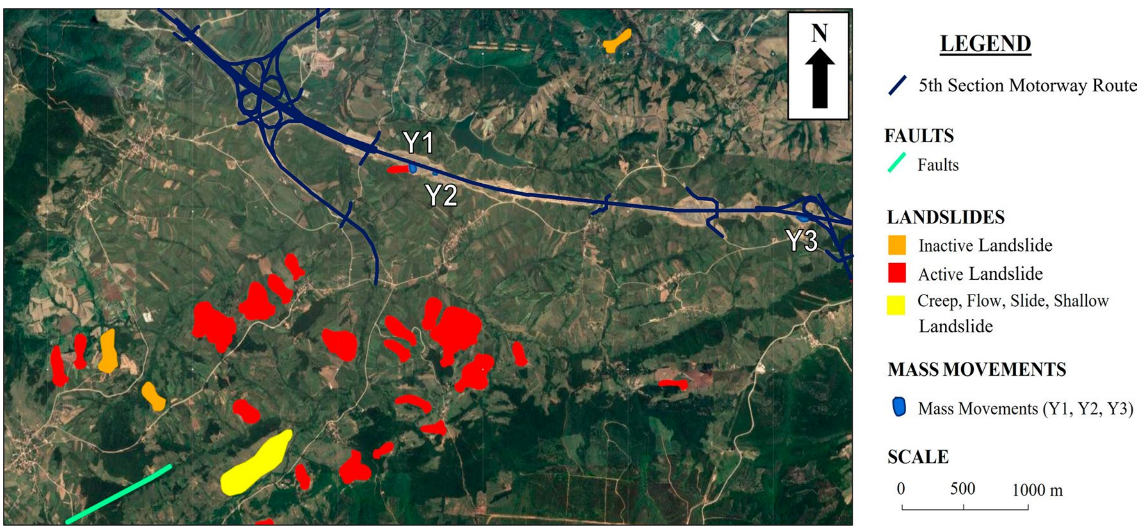

Fig. 4 Active faults and landslides of the region according to General Directorate of Mineral Research and Exploration (MTA) GeoScience MapViewer (Department of Scientific Documentation and Publicity, 2016) and Y1, Y2, and Y3 mass movements along the 5th Section Motorway Route

Peak Ground Acceleration (PGA), Local Soil Coefficient, and Spectral Acceleration Coefficients (S_s, S_1, S_{DS}, S_{D1}) for the slope to be analyzed in the study area have been determined according to the TER (2018) and Turkiye Earthquake Hazard Map prepared by the Ministry of Interior, Disaster and Emergency Management, Earthquake Department (AFAD 2019). To calculate the Peak Ground Acceleration (PGA), Local Soil Coefficient, and Spectral Acceleration Coefficients (S_s, S_1, S_{DS}, S_{D1}) values of the study area, the coordinate information of the region was entered into the Turkiye Earthquake Hazard Maps Interactive Web Application (TEHMIWA, 2018) and a report was created by the application. According to this report, Seismic Ground Motion Values are DD-3 that characterize frequent earthquake ground motions with a 50% probability of exceeding the spectral magnitudes within 50 years and equivalent to the return period of 72 years.

Materials and methods

To determine the index properties of the cut materials, field and laboratory studies were carried out in the regions where mass movements occur. Laboratory and field tests, such as specific bulk density (γ_n), sieve analysis, Atterberg limits, standard proctor test, CBR (California Bearing Ratio), and point loading tests, should be done in the design of the cut slopes according to the Disaster Regulations for Motorway Engineering Structures (Part 5/Matter 48) (Ministry of Public Works and Settlement 2006). Laboratory and field tests to evaluate the study area were carried out taking into consideration the regulations. Locations, classifications, numbering, spacing, types and characteristics of the cut materials, and water conditions of the discontinuities affecting the stability of the slope in the sections not covered by vegetation or weathered/soiled levels have been determined by field explorations. Rock mass classification of the units was carried out using RQD, GSI and RMR_{89} rock classification methods (Çakıner 2021).

RocData software (Rocscience 2004) was used to determine the parameter values of the geo-materials which are based on laboratory and field tests. The strength parameters of Y1, Y2, and Y3 mass movements were determined. Mohr–Coulomb shear strength outcomes were used in the analyses. Strength parameter values determined with RocData software were used as input for Slide2 numerical analysis programs. Stability analyses using the geological–geotechnical parameters determined by drillings, and field and literature studies were evaluated with the Rocscience Slide2 (2004) software using Bishop (1955), Janbu (1957, 1973) and Spencer (1967) methods according to the limit equilibrium method. Information about strength parameters and the factor of safety values is given in the sections drawn with Slide2 software. To provide a comprehensive understanding of the strength parameters and factor of safety values, this study obtained information from the previous studies using Slide2 software. Within the scope of this study, the conditions specified in the Republic of Turkiye General Directorate of Highways Technical Specification and technical circulars (General Directorate of Highways) were taken into consideration while determining design values for slope stabilization. While evaluating the environmental characteristics, the test pits and drilling data were obtained closest to the kilometers where mass movements occurred.

The effect of precipitation on the stability problems of the slopes was studied by calculating the meteorological water balance of the region using the method of Penman (1948), and the mechanism of the occurrence of mass movement was explained in the combination of environmental parameters and water ratio. The stability analysis of slopes where mass movement occurred was analyzed with the environmental parameters established for the slope geometry proposed in the original project design case using Rocscience Slide2 (2004) software. An initial analysis showed that the slopes were stable within the specified environmental parameters. Although the slopes defined in the project appeared to be stable in the model calculations, geotechnical solutions for these slopes were initiated by calculating the design parameters of slopes with mass movement due to mass movements on some slopes using the back-analysis method. After understanding the reasons for the weathering of the slopes and calculating the values of the back-analysis method, geotechnical precautions, such as pile retaining walls, slope stabilization, etc., were proposed with new slope arrangements on the slopes where mass movements were observed. As a result of this study, the proposed solutions and precautions were implemented in the project.

Subsurface boreholes

To determine the geotechnical properties of the units belonging to the mass movements in the study area, the boreholes with elevations and locations shown in Table 2 were drilled (Fig. 5). The drilling cores were examined, and a geological assessment was made from the drilling cores. Detailed information and data regarding the strength, crack conditions, and weathering of the units obtained from boreholes are provided below (Fig. 5). Boreholes drilled in close proximity to the mass movement areas confirm the presence of the Ypresian Korucu Formation. The YSK 170 + 212 and YSK 170 + 710 cut slopes exhibit intensive alternating bedding of claystone and siltstone units. Field and laboratory studies indicate the presence of a hard, low–medium plasticity silty clay with a sandy gravel, yellowish brown composition at the base of the region. Lower levels of the boreholes reveal fractured siltstone, claystone, and shale units, showing slight to moderate weathering, weak strength, and occasional sandstone interlayers. In the YSK 175 + 330 cut slope, the Korucu Formation units at lower levels exhibit moderate to high weathering, weak strength, and intense fracturing in the upper levels. Claystone is the dominant lithology in this cut, although there are partial intercalations of sandstone and siltstone.

TCR (total core recovery)—RQD (rock quality designation) test result graphics of rock cores made by TTS Engineering (2018) in the study area are given in detail in Fig. 6. For YSK 170 + 212 borehole, the average TCR value in the claystone–siltstone unit was calculated as 90% and the average RQD value was calculated as 18%. According to the average RQD value, the rock class is very poor. The average TCR value in rock cores for the YSK 170 + 710 was calculated as 97%. Since there was no sample longer than 10 cm, the RQD value could not be obtained. In the TCR–RQD evaluation of the rock cores for the YSK 175 + 330 borehole the TCR was 100% and the average RQD value was 34% throughout the drilling. According to the average RQD value the rock class was determined as poor.

Atterberg (1911) limits and sieve analysis tests were performed on undisturbed soil samples taken from the cut slopes to define soil classes. As a result of the tests, the soil classes of the SPT-1, SPT-2, and SPT-3 samples taken from the YSK 170 + 212 borehole was determined as CL (low

Table 2 Sieve analysis, Atterberg limits, unit weight and point loading test results of YSK 170 + 212, YSK 170 + 710 and YSK 175 + 330 boreholes

Borehole No	Depth (m)	GWL (m)	Lithology	Sample Information		Unit Weight	Point Load	Formation Name	Sample Information		Sieve Analysis		Liquid Limit, Plastic Limit, Plasticity Index			Soil Classification
				Sample No	Depth (m)	γ_n (gr/cm^3)	Is_{50} (MPa)		Sample No	Depth (m)	4 (%)	-200 (%)	LL (%)	PL (%)	PI (%)	
YSK 170+212	20	7.2	4.6 m of soil, followed by highly weathered, weak-strength Claystone	K1	4.50-5.00	2.169	0.90	Korucu Formation	SPT-1	1.50-1.95	1.98	87.05	41	13	28	CL
				K2	6.00-7.00	2.211	0.24		SPT-2	3.00-3.95	2.39	78.77	29	16	13	CL
				K3	10.50-11.00	2.138	0.08		SPT-3	4.50-4.95	1.85	91.95	43	14	29	CL
				K4	12.50-13.50	2.261	0.08		SPT-4	6.00-6.65	*Since the samples were insufficient for the experiments, the relevant soil tests could not be performed.					
				K5	15.00-16.00	2.396	0.14									
				K6	18.50-19.00	2.359	0.31									
YSK 170+710	40	18.7	Moderate-fractured, moderately-highly weathered, weak-strength Claystone	K1	3.00-4.50	2.074	0.36		SPT-1	1.50-1.95	0	97.1	45	14	31	CL
				K2	7.50-8.50	2.153	0.36									
				K3	10.50-11.50	2.303	0.50									
				K4	15.50-16.50	2.295	0.32									
				K5	17.50-18.50	2.290	1.06									
				K6	23.50-24.00	2.327	0.64									
				K7	27.50-28.50	2.292	1.72									
				K8	38.50-39.00	2.221	0.26									
				K9	36.00-37.00	2.249	0.78									

Table 2 (continued)

Borehole No	Depth (m)	GWL (m)	Lithology	Sample Information		Unit Weight	Point Load	Formation Name	Sample Information		Sieve Analysis		Liquid Limit, Plastic Limit, Plasticity Index			Soil Classification
				Sample No	Depth (m)	γ_n (gr/cm^3)	Is_{50} (MPa)		Sample No	Depth (m)	4	-200	LL	PL	PI	
											(%)	(%)	(%)	(%)	(%)	
YSK 175+330	32	3.4	0.8 m of soil, followed by intense fractured, moderately weathered, weak strength Claystone	L1	1.00-2.00	1.900	0.07		–							
				L2	6.00-7.00	1.950	0.16									
				L3	10.00-11.00	2.000	0.25									
				L4	18.00-19.00	2.100	0.29									
				L5	25.00-26.00	2.050	0.27									
				L6	30.00-31.00	2.220	0.45									

plasticity clay) according to the Casagrande (1932) Plasticity Chart (Table 2). This soil class can be defined as low plasticity sandy/sandy silty clay. As a result of the sieve analysis and Atterberg limit values performed on the SPT-1 sample taken from the YSK 170 + 710 borehole, it was observed that the soil was CL (low plasticity clay) (Table 2, Fig. 7).

In order to determine the physical and mechanical properties of the rock units in the mass movement area, unit weight and point load tests were conducted (Table 2). The YSK 170 + 212 cut slope borehole exhibited unit weight values ranging from 20.974 to 23.497 kN/m^3 and point load strength index values ranging from 0.08 to 0.90 MPa (Table 2). It falls under the category of weak-strength rocks with an average strength of 0.29 MPa (Bieniawski 1975). For the YSK 170 + 710 cut slope boreholes, the point load strength index values ranged from 0.26 to 1.72 MPa (Table 2), indicating a medium-strong rock class with an average strength of 0.67 MPa (Bieniawski 1975). The unit weight values ranged from 20.339 to 22.820 kN/m^3 (Table 2). In the YSK 175 + 330 cut slope borehole, the unit weight test results ranged from 18.633 to 21.770 kN/m^3 between depths of 1.00 to 31.00 m, and the point load strength index values ranged from 0.07 to 0.45 MPa (Table 2). This indicates a weak-strength rock class with an average strength of 0.25 MPa (Bieniawski 1975).

The empirical determination of point load strength index values and uniaxial compressive strength is used in the assessment of rock stability. The rock mass classification proposed by Bieniawski (1989) was employed to calculate the stability analysis parameters for the Y1, Y2, and Y3 mass movements. According to this classification, if the average point load strength index value is less than 1–2 MPa, uniaxial compressive strength values should be utilized. Since the average corrected point load values for YSK 170 + 212, YSK 170 + 710, and YSK 175 + 330 boreholes were 0.29 MPa, 0.67 MPa, and 0.25 MPa, respectively, uniaxial compression test results were required. As uniaxial compressive strength tests could not be conducted on the rock samples of Y1, Y2, and Y3 mass movements, the point load strength index values were converted using empirical correlations based on the uniaxial compressive test results by using Eq. (1).

$$\sigma_c = K \times I_{s(50)} \tag{1}$$

Within the scope of this study, to determine the index-to-strength conversion factor (K) of the study area, the relationship between all uniaxial compression test values and point loading index values, which were taken as a sample from Korucu Formation, 5th Section of the Northern Marmara Motorway, was shown on separate graphs (Fig. 8a,b) made using Microsoft Excel. The smallest suggested number for the index-to strength conversion factor (K), which is 20, was selected enabling a potential uniaxial compression value to

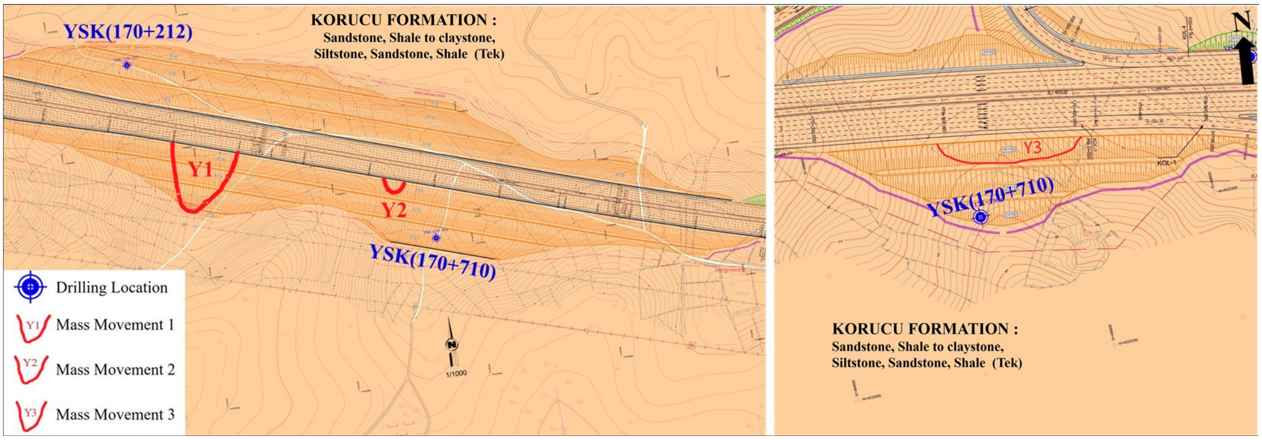

Fig. 5 Location of boring logs and Y1–Y2–Y3 mass movements

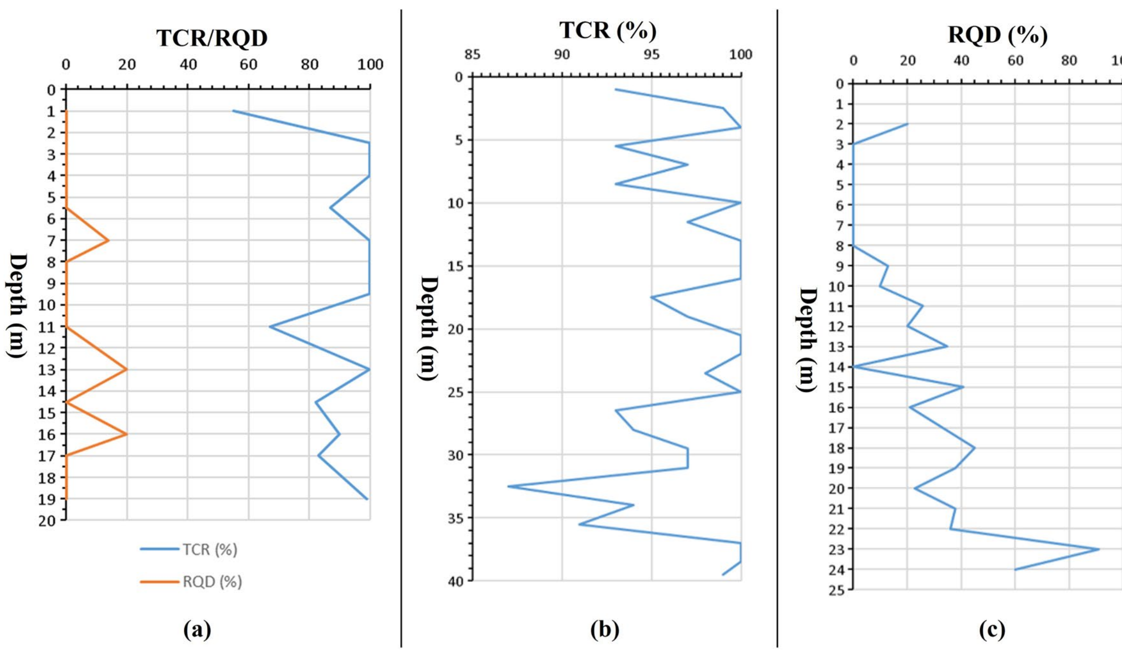

Fig. 6 **a** TCR and RQD values for YSK 170 + 212 boring log, **b** TCR values for YSK 170 + 710 boring log, **c** RQD values for YSK 175 + 330 boring log

be calculated via Eq. (1). The possible uniaxial compressive strength results of the rock calculated with Eq. (1) and the uniaxial compressive test results were evaluated together. It was observed that the possible uniaxial compressive test results and uniaxial compressive test data were compatible with each other; thus, further justification for K value being selected as 20 for this study (Fig. 8c).

As a result of this study, while stability analyses were performed for Y1, Y2, and Y3 mass movements, Eq. (1) was used for σ_c values in parameter determination stages. According to this approach, when calculating the stability for the Y1 mass movement, the average value of the corrected point load strength values of the YSK 170 + 212 cut slope borehole, 0.29 MPa, was evaluated with Eq. (1), and the uniaxial compression value of the rock was taken as 5.83 MPa (≈ 6 MPa). The average of the corrected point load strength values of the YSK 170 + 710 cut slope borehole was used for the Y2 stability analysis. The average of the corrected point load strength values of the YSK 170 + 330 cut was used for the Y3 stability analysis. According to these results, the uniaxial compression values of the rock were taken as 15.09 MPa (≈ 15 MPa) for the Y2 mass movement and 3.20 MPa (≈ 3 MPa) for the Y3 mass movement.

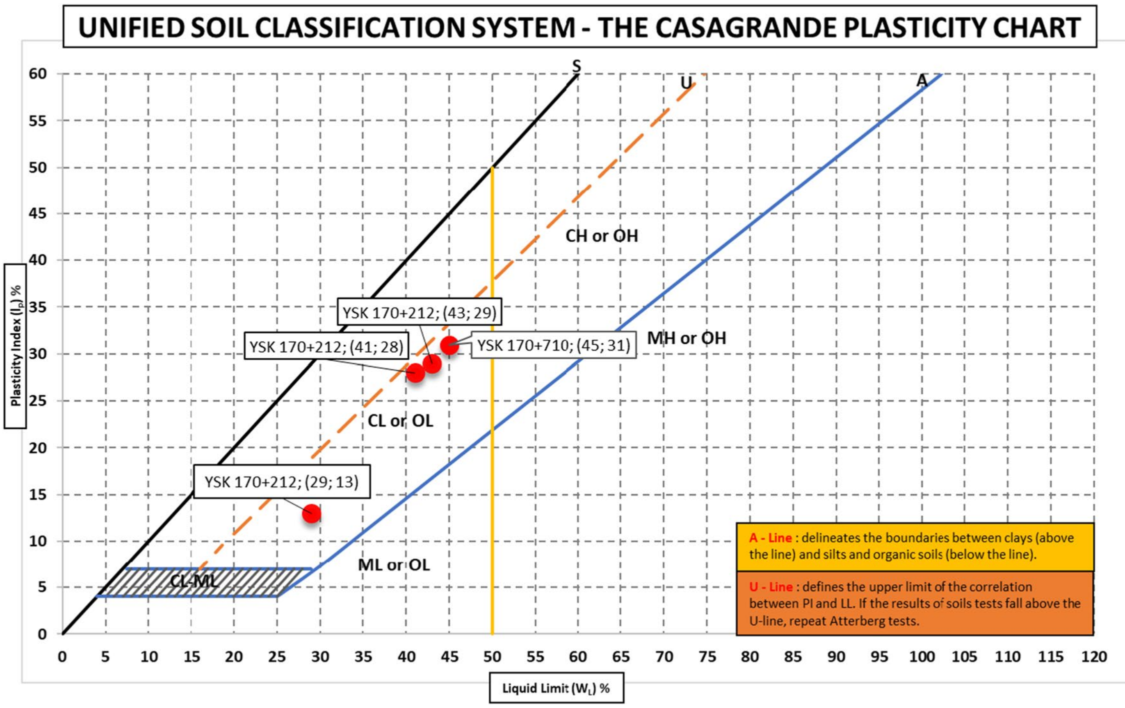

Fig. 7 Evaluation of YSK 170 + 212 and YSK 170 + 710 boreholes according to the unified soil classification plasticity chart

Field studies

Field studies were carried out for investigation of mass movements. The purpose of the field study is to determine the surface features, cut slope, vegetation, climate, water condition, and geological and lithological structures of the area where mass movements occur. The depth of the slip surface, the type of the slip movement, the slip axis, direction, distributions, classifications, and dimensions of mass movements were determined to define mass movements on the slopes. Aerial photographs were also used to increase the field of view during field studies (Fig. 9).

The slope movement, which took place in the YSK 170 + 212 cut slope and is called mass movement 1 (Y1) in this study, occurred between km: 170 + 300–170 + 400 (Fig. 9a, b). At the termination zone, the refuge and right side of the carriageway were elevated by 80 cm and formed the toe. Cracks had formed in a section of about 3 m due to slipping at the top of the landslide (Fig. 9a). The investigations conducted on the mass movement, revealed its impact across a horizontal span of 100 m. The observed characteristics identified the mass movement as a rotational slip (landslide) type (Wicander and Monroe 2005). The study area is within a zone of active tectonic activity. As a result of the tectonic activity in the region, the sedimentary units are frequently fractured and cracked. The development of discontinuity planes through the formation of cracks and fractures in sedimentary rocks is attributed to tectonic activity. These geological processes enable the transportation and transmission of water, within the rock formations, contributing to the creation of fractured and cracked rock aquifers. In the environmental evaluation made with field observations and laboratory test results, it was understood that the cause of the landslide was the cracks in the claystone that transmitted water, the micro-cracks in the clay, and the discontinuities formed by the development of these cracks over time. In the studies, it was observed that the micro-cracks that occurred in the clay consolidated over time and formed the slip surface. As a result of the friction generated by the clay unit, the slope is capable of self-sustained movement along the sliding surface for a certain duration. Subsequently, the frictional resistance on the sliding surface is surpassed, leading to occurrence of a landslide. The slope movement, which took place in the YSK 170 + 710 cut slope and is called mass movement 2 (Y2) occurred at kilometer km: 170 + 640 (Fig. 9c). In the field studies, it was determined that the type of mass movement was a translational slide. A translational slide took place in the contact zone between vegetable soil and claystone on the first slope area. The first slope surface has a height of 10 m from the slope base. The slope movement, which took place in the YSK 175 + 330 cut and is called mass movement 3 (Y3) in this study, occurred at kilometer km: 175 + 297–175 + 463 (Fig. 9d). Ruptures and local flows occurred on the slope surface. According to the field observation, it was determined that the type of mass movement was a flow. While yellow-colored clay material

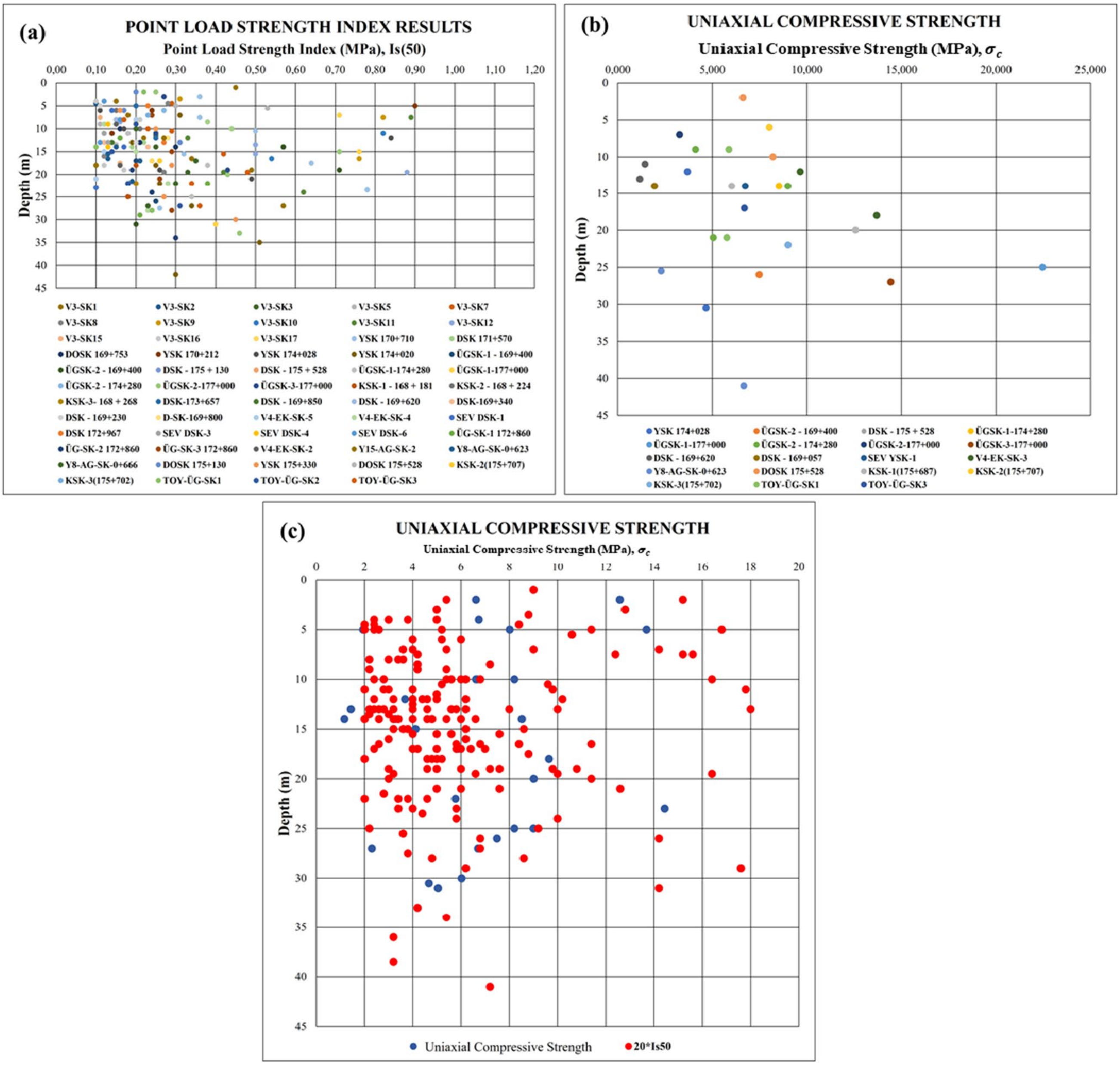

Fig. 8 **a** Relationship between the point-load index and depth for Korucu Formation, **b** Relationship between uniaxial compressive strength and depth for Korucu Formation, **c** Correlation between uniaxial compressive strength values and depth in terms of uniaxial compressive strength test results, point load index test results and the smallest suggested number for the index-to-strength conversion factor (K)

was observed in the first 2 m of the flow zone, intensely fractured claystone was observed in the next 10 m (Fig. 9d). It has been determined that the flow type mass movement occurring between 175 + 297 and 175 + 463 kms was caused by water leaks (pool, garden irrigation, waste, clean water leaks, etc.) originating from a ranch house on the top of the slope. Correspondingly, the dwelling's pool water had soaked up the soil along with the groundwater level. The soil saturated with water, reached the liquid limit and has developed a flow-type movement. The Google Earth view of the spatial relationship between the mass movement and the water recharge point that triggers the movement is shown in Fig. 10.

Slope stability and improvement studies

Slope stability studies of mass movements that occur with flow and slides on the cut slopes on the 5th section of the

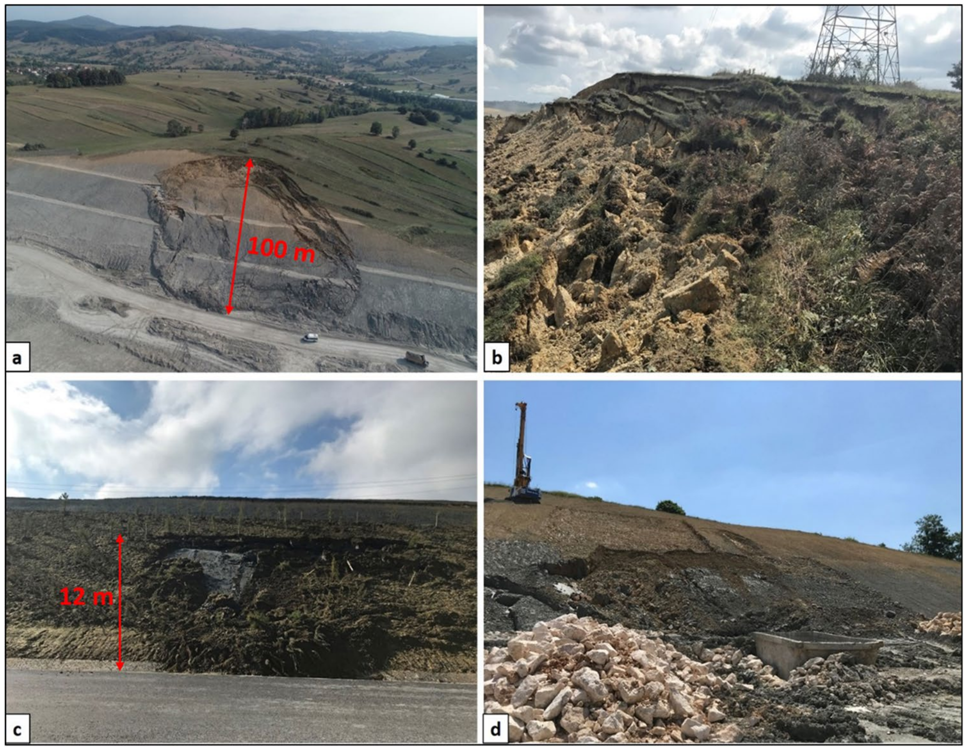

Fig. 9 **a, b** Front and side view of the rotational slip (landslide) type mass movement occurring in the km: 170 + 300–170 + 400, **c** Front view of translational slide-type mass movement at km: 170 + 640, **d** Side view of flow-type mass movement occurring between km: 175 + 297–175 + 463 kms

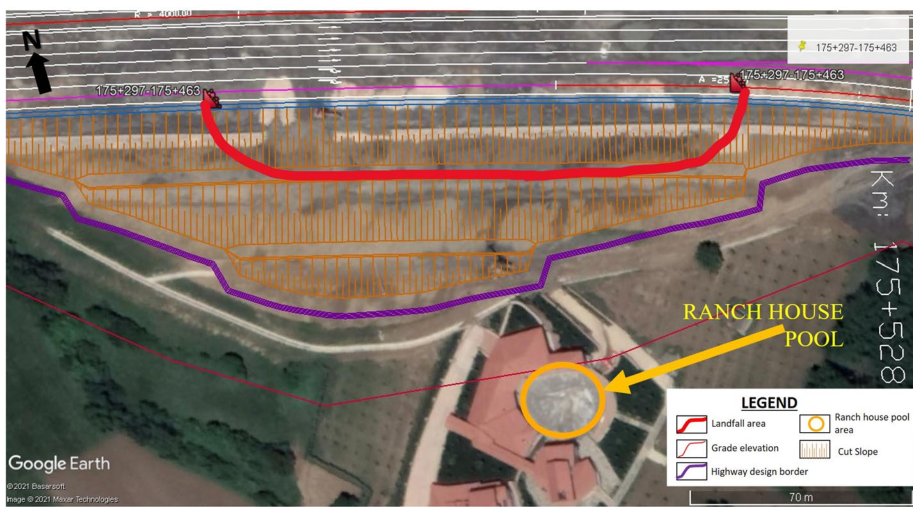

Fig. 10 Image of the location of the mass movement and the water recharge point that caused the mass movement in kilometers between 175 + 297 and 175 + 463 (Google Earth 2020)

Northern Marmara Motorway have been investigated. Accordingly, suggestions were made for the improvement of the slopes.

A transmission tower exists at the top of the slope where Y1 mass movement occurred. Therefore, while performing the slope stability improvement analysis, surcharge load is added to the cross-section in the Slide2 software for the transmission tower (Fig. 11). When the laboratory test results are associated with empirical correlations and the slope is evaluated, it is observed that the factor of safety of the slope is FS = 1.25 in the first design situation (Fig. 11). The determined value of the safety factor (FS = 1.25) is below the value of the safety factor (FS ≥ 1.50) of the long-term static analyses for cut slopes. Thus, slope stability improvement is required for the Y1 mass movement.

When the area was evaluated and correlated with the empirical correlations, the laboratory test results for the Y3 mass movement showed that the factor of safety value (FS = 2.539) of the slope in the initial design condition was sufficient for the slope to remain stable (Fig. 12).

Although the design shown in Fig. 12 looks stable, the flow-type mass movement has developed in the slope. The claystone in the Y3 slope was detailed with weathering products instead of a single unit and the design

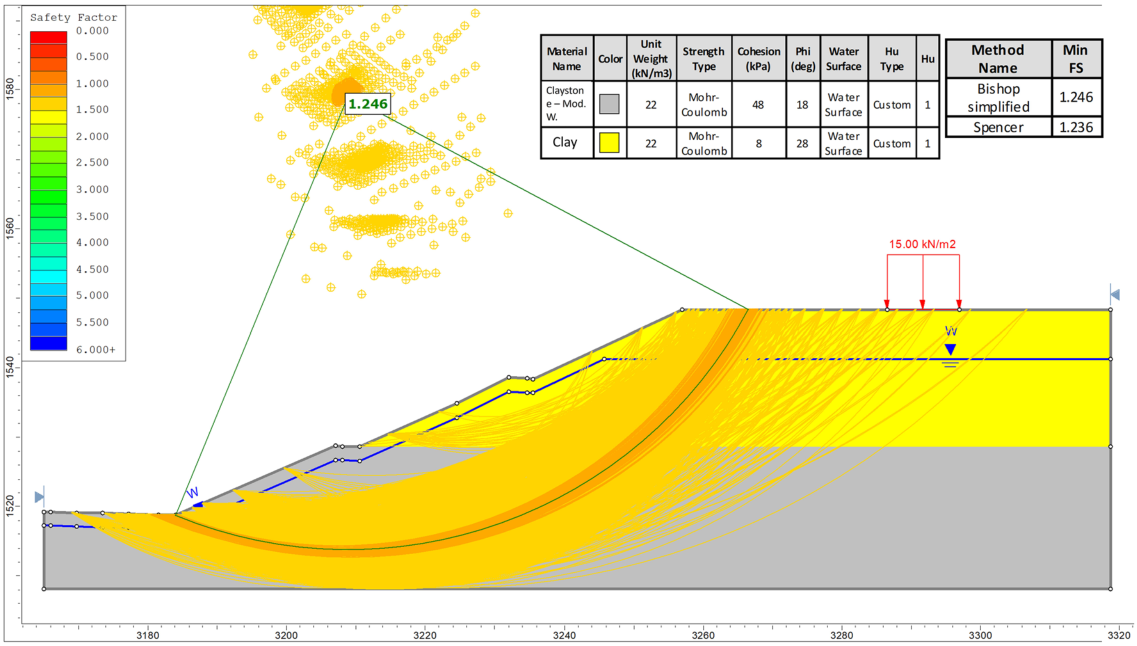

Fig. 11 Slope stability analysis of km: 170 + 300–170 + 400 (Y1) mass movement before slipping (Static Condition)

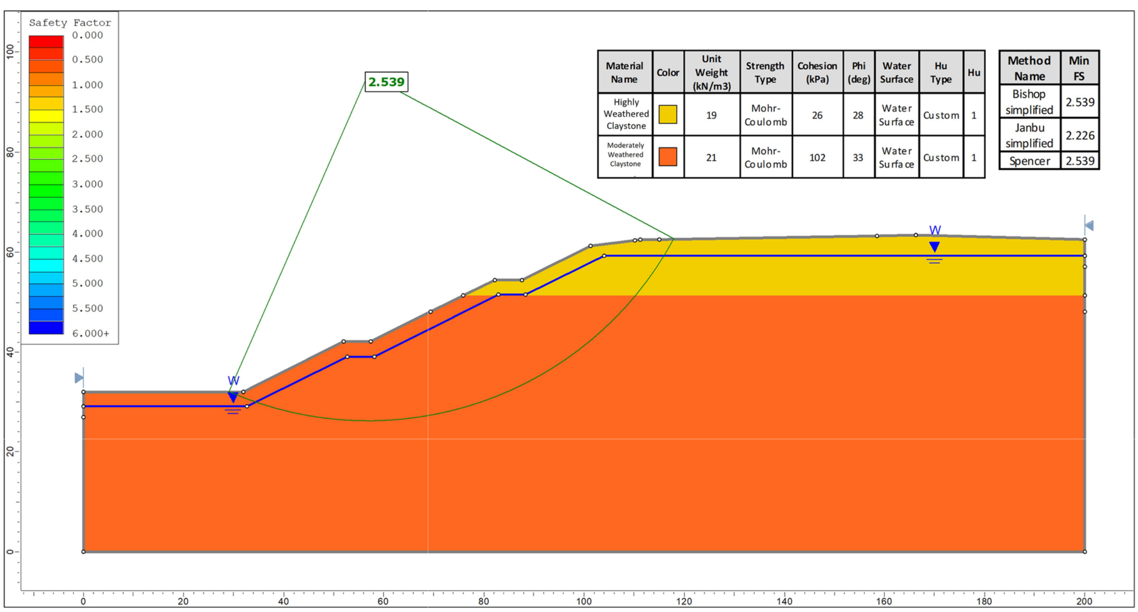

Fig. 12 Initial state analysis of slope geometry where Y3 mass movement develops, drawn in Slide2 software ($D = 0$)

parameters of each weathering state were determined to prevent the development of the movement over time and examine the long-term stability of the slope for shear-type movement and ensure this stability. This design aims to hinder mass movement development over time, ensuring long-term stability against sliding-type motion and promoting overall structural stability. Design parameters have been determined for both moderately and highly weathered conditions (Table 3). To facilitate this analysis, the material found in the upper strata of the study area, characterized as highly weathered claystone, was utilized in the calculations. It was evaluated as moderately weathered claystone in the units located at the lower levels.

Table 3 RMR classification parameters and ratings for Y1, Y2, and Y3 claystone–siltstone units

Mass movements no	Y1	Y2	Y3	
Weathering	Mod. W	Mod. W	Mod. W	Highly W
Parameter	(Rating)			
Uniaxial Compression Strength, MPa	2	2	2	1
Drill core quality, RQD (%)	3	3	8	3
Spacing of discontinuities	5	5	8	5
Groundwater, General Conditions—Completely Dry	15	15	15	15
Discontinuity length (persistence)	2	2	2	1
Separation (aperture)	4	4	4	1
Roughness—Slightly rough	3	3	3	3
Infilling (gouge)—Hard filling > 5 mm	2	2	2	2
Weathering	3	3	3	1

Determination of strength parameters for Y1, Y2, and Y3 mass movements

Calculations of strength parameters for the clay unit of Y1

The long-term drained shear strength parameters in the clay unit, depending on the plasticity index, pre-consolidation pressure of clay, geological stresses, and angle of internal friction were determined with equations proposed by Terzaghi et al. (1996) and Mesri and Abdel-Ghaffar (1993) (Fig. 13). The friction angle (ϕ') depending on the plasticity index value of the clay was determined as 28° (Fig. 13a). The m parameter depending on the plasticity index value is found as 0.74 to determine the cohesion value (Fig. 13b).

The relationship between the peak shear strength value and the effective normal stress and water content value is defined by the empirical relationship given by Mesri and Ghaffar (1993) with Eq. (2) for normally consolidated clays. The following symbols are used in Eq. (2): $\phi\prime$: friction angle, $c\prime$: cohesion intercept, m: parameter defining curvature of intact strength envelope, $\sigma_p\prime$: preconsolidation pressure, $\sigma_n\prime$: effective normal stress.

$$\frac{c\prime}{\sigma_{\mathrm{p}}\prime} = (1 - m)\tan\phi\prime\left(\frac{\sigma_{\mathrm{p}}\prime}{\sigma_{\mathrm{n}}\prime}\right)^{-\mathrm{m}} \quad (2)$$

As a result of the calculation, the cohesion intercept value is $c\prime = 7.603 \approx 8$ kPa.

Calculations of strength parameters for Y1 (claystone–siltstone-moderate weathered), Y2 (claystone-moderate weathered) and Y3 (claystone-moderate and highly weathered) units

The RMR classification was made according to the field condition using the average values of the laboratory results of the YSK 170 + 212, YSK 170 + 710 and YSK 175 + 300 boreholes for the claystone-siltstone and claystone units of the Korucu Formation, in which the Y1 and Y3 mass movements took place. In situ strength parameters were calculated

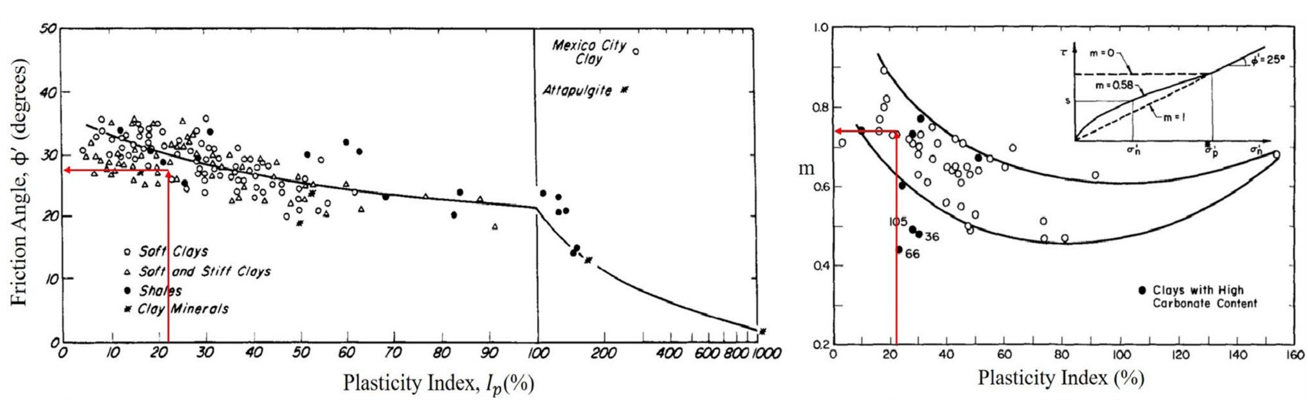

Fig. 13 **a** The relationship between values of friction angle for clays of various compositions as reflected in plasticity index (Terzaghi et al. 1996) and **b** Values of m in terms of plasticity index (Mesri and Ghaffar 1993)

with RocData software. RMR classification parameters for Y1, Y2, and Y3 are shown in Table 3.

As a result of the evaluations, the RMR_{89} value was calculated as 39 for the Y1 and Y2 claystone–siltstone unit, 47 for the moderately weathered claystone unit of Y3, and 32 for the highly weathered claystone unit of Y3. If the rock mass rating is determined with RMR_{89}, it is recommended to calculate the geological strength index (GSI) value with Eq. (3) (Ulusay and Sönmez 2006; Hoek 1994).

$$GSI = RMR_{89} - 5 \quad (3)$$

The GSI value was obtained as 34 for Y1 and Y2 mass movement area, 42 for the moderately weathered claystone unit of Y3 area and 27 for the highly weathered claystone unit of Y3 mass movement area. After calculating the RMR values, input and output data depending on field observations and boreholes are given in Table 4 to determine the in situ strength parameter values with Rocscience RocData (2004) software.

Determining parameters with back analysis method for Y1 mass movement

Due to the mass movement in the sections determined to be safe in the previous calculations made in the study area, in situ strength parameters were also calculated by the back-analysis method. For this purpose, the slope geometry before the sliding motion has been created with the Rocscience Slide2 (2004) software as a first step. The groundwater level in slope geometry was assigned as 7.2 m based on YSK 170 + 212 drilling. For the pylon at the top of the slope, a 15 kN/m^2 surcharge load has been added to the top of the slope in the software. In the analysis, slip parameter values were sought for FS = 1 in the critical slip circle and the value of c was found to be 0 kPa, the value of ϕ was found to be 29° (Fig. 14).

In the analysis, the result strength parameters were assigned as the values given in Table 5 by evaluating all the studies done in the field and laboratory.

Stability analysis for km: 170 + 300–170 + 400 (Y1) and km: 175 + 297–175 + 463 (Y3) mass movements

The factor of safety of Y1 and Y3, in which sliding and flow type movements developed, was computed using Bishop, Janbu and Spencer methods (Bishop 1955; Janbu 1957, 1973; Spencer 1967) in RocScience Slide2 (2004) software. After that, new slope geometries were designed and analyzed based on field observations with the determined strength parameters of the landslide condition.

The claystone unit belonging to the Ypresian Korucu Formation differs within itself in terms of weathering. This situation was reflected in the model, the slip parameter values determined in Table 5 were assigned based on the engineering geology evaluation, and long-term stability on the slope was investigated. The static condition analysis of the Y1 is given in Fig. 15.

The rock disturbance that could occur after excavation in the Y3 mass movement and due to the weathering effect depending on time has been evaluated for $D = 0.3$ and $D = 0.5$, and stability analyses have been made according to the design parameters finalized in Table 5 (Fig. 16).

In analysis, it has been understood that in the case of $D = 0.3$ disturbance, the slope stability is provided (Bishop FS = 1.267, Janbu FS = 1.163, Spencer FS = 1.268) for slip-type movement, but in the case of $D = 0.5$ disturbance, the slope will not be stable (Bishop FS = 0.899, Janbu FS = 0.822, Spencer FS = 0.900) for slip-type movement and rotational slip (landslide) type mass movement will develop on the slope (Fig. 16). When the environment is evaluated in terms of long-term stability (FS ≥ 1.50), it is seen that there is no slope safety for the disturbance factors ($D = 0.3$ and $D = 0.5$). For this reason, the long-term stability of the slope was considered in the unity of flow and slip-type movement, and analyses were made by bringing the groundwater level as close as possible to the slope surface due to the risk of water leakage from the pool of the ranch house on the slope.

Table 4 RocData parameters for Y1, Y2 and Y3 mass movements

Mass Mov. No	Rock Properties	RQD (%)	UCS (MPa)	m_i	D	GSI	MR	γ_n (kN/m^3)	c (kPa)	ϕ (°)
Y1	Moderately Weathered	18	6	4.0	0.7	34	250	22	48	18
Y2	Moderately Weathered	–	15	4.0	0.7	34	250	22	82	22
Y3	Moderately Weathered	40	7	4.5	0	42	275	21	102	33
	Highly Weathered	17	3	4.0	0	27	250	19	26	28
	Highly Weathered-Disturbed	17	3	3.0	0.3	27	225	19	19	22
	Highly Weathered-Disturbed	17	3	2.0	0.5	27	200	19	13	17

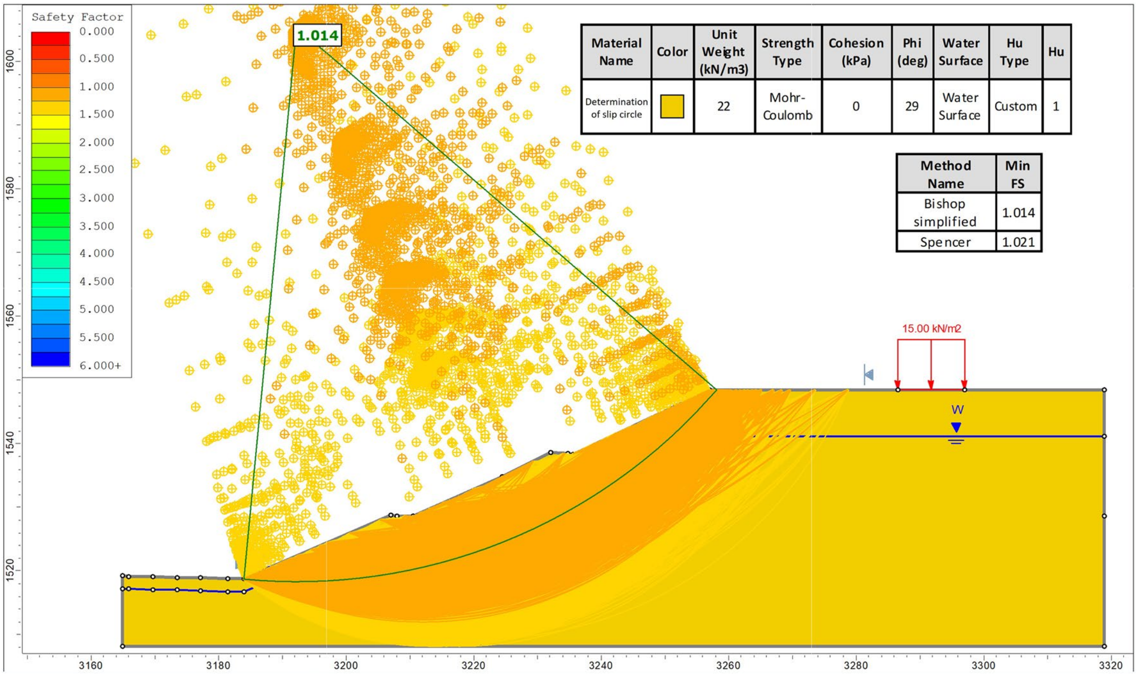

Fig. 14 Image of the process of determining the slip plane parameters

Table 5 Parameters used before improvement applications in Slide2 analysis

Lithology	Material Model	c (kPa)	ϕ (°)	γ_{sat} (kN/m^3)
Slip Plane	Back Analysis	0	29	22
Clay	Mohr–Coulomb	8	28	
Claystone-Siltstone	Mohr–Coulomb	48	18	

Improvements of km: 170 + 300–170 + 400 (Y1) and km: 175 + 297–175 + 463 (Y3) mass movements

A pile retaining wall is proposed to improve the Y1 mass movement. The position of the piles was determined according to the balance center of the sliding mass and the parameters determined before the slip and given in Table 5 for clay and claystone were used in the analysis model. For the analyses, the relationship between slope height and the factor of safety was examined. Due to the presence of a transmission tower at the top of the slope, the appropriate slope angle was investigated. As a result of analyses, the slope angle designed as 22° has been reduced to 17° with the improvements. The first and third cut slope ratio has been rearranged to be 3:1 (horizontal:vertical) and the second one is to be 3.5:1 (horizontal:vertical).

The observed thickness of the disturbed mass flowing in the region where the Y3 flow-type mass movement occurs is 5 m. As a result of the cut excavation, the cracks in the damaged pool of the building were repaired, the dirty–clean water leaks were prevented, and the water originating from the building was prevented from reaching the slope. An artificial nature design (surface protection with greening, afforestation, etc.) was made on the slope surface and water infiltration from the slope surface into the ground was tried to be kept at a minimum level. Suggested stability improvements for Y1 and Y3 mass movements are given in Table 6.

In the analysis conducted to evaluate the factor of safety values following the implementation of stability improvement techniques on the Y3 slope, specific assumptions have been considered regarding the rip-rap stone-rock material to be utilized on the 1st and 2nd slope surfaces. In accordance with these assumptions, the following values have been adopted: $c = 5$ kPa, $\phi = 35°$, and $\gamma = 20$ kN/m^3, as referenced in the works of Budhu (2011) and Carter and Bentley (1991).

As a result of the suggested stability improvements techniques, it has been observed that the slope maintains its stability in static (Fig. 17) and dynamic (Fig. 18) conditions in the case of $D = 0.3$ and $D = 0.5$ disturbances.

In the dynamic condition analysis, map spectral acceleration coefficients (S_s and S_1), peak ground acceleration and velocity (PGA and PGV), PGA_{ground}, and horizontal seismic coefficient (k_h) were determined (Table 7) with Türkiye Earthquake Hazard Map Interactive Web Application (TEHMIWA, 2018).

Reconstructed slope geometry and the factor of safety values of the analysis results of the proposed pile retaining wall improvements created with Slide2 (2004) software are provided in Table 8.

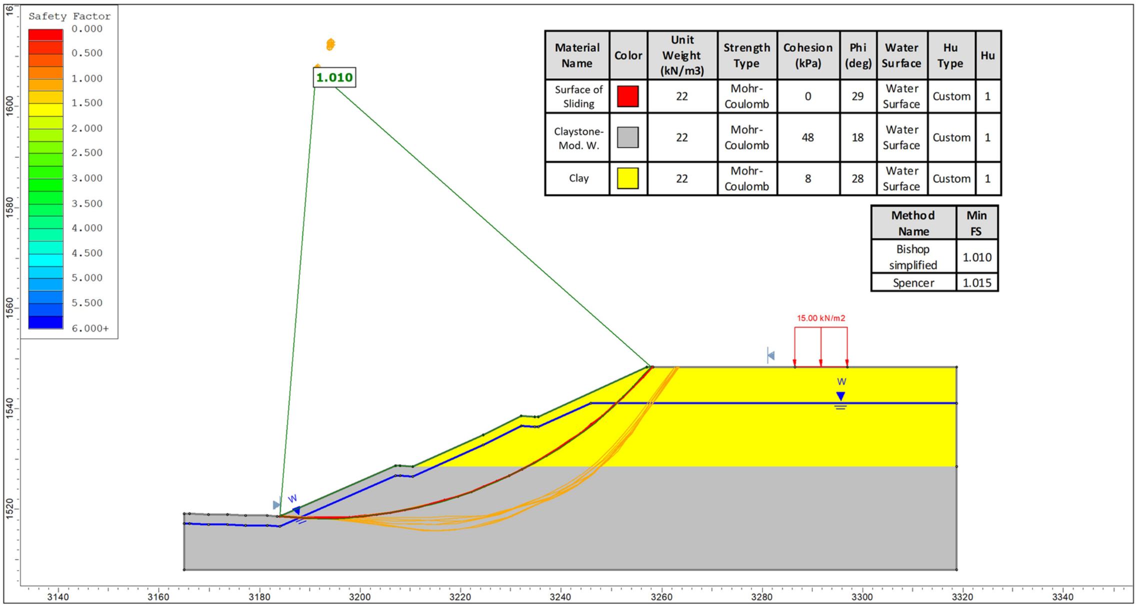

Fig. 15 Sliding plane finding with back analysis method of km: 170 + 300–170 + 400 (Y1) mass movement and slope stability analysis after strength parameters are inputted in Slide2 software (Static Condition)

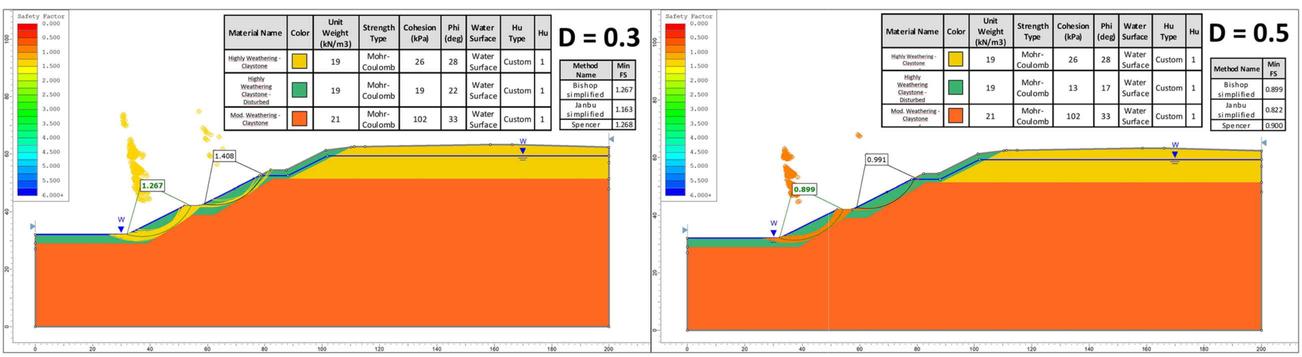

Fig. 16 Analysis of the possibility of sliding-type movement in slope geometry with Slide2 after the Y3 mass movement (*D* = 0.3 and 0.5)

Table 6 Suggested stability improvements for Y1 and Y3 slope failures

Mass Movement No	Suggested Stability Improvement Techniques	
Y1	Stage 1: It has been suggested that 29 pieces of L = 15 m length φ = 1.20 m diameter piled (Concrete class: C30/37, Reinforcement: B420C, Pile Cover: 7.5 cm) retaining wall application should be applied on the lowest bench level	Stage 2: It has been suggested that 21 pieces of L = 20 m length φ = 1.20 m diameter piled (Concrete class: C30/37, Reinforcement: B420C, Pile Cover: 7.5 cm) retaining wall application should be applied on the uppermost bench adjacent to the top of the slope
Y3	1. Prevention of water leakage originating from the dwelling 2. Adding drainage to the slope 3. Surface protection & Ecological Restoration or Rip-Rap application 4. Retaining structures for dynamic condition 5. Support items and measures	

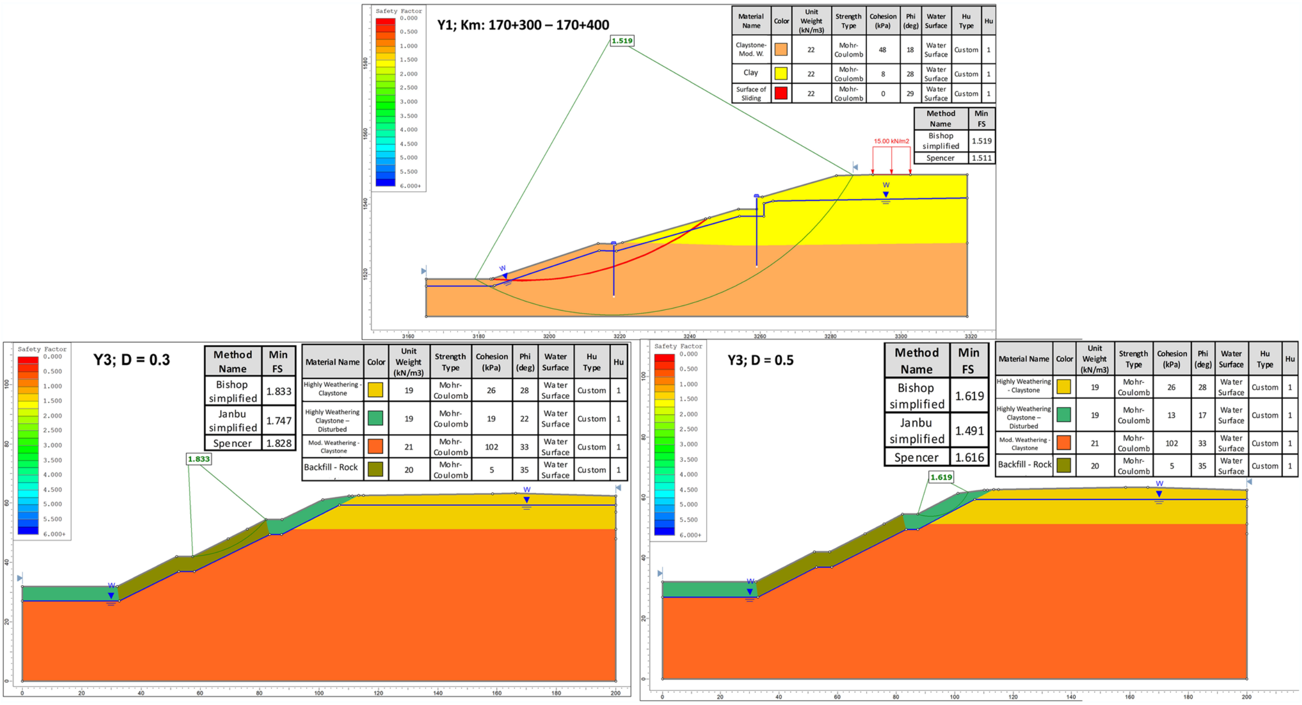

Fig. 17 Static condition analysis of slope improvement in Y1 and Y3 mass movements

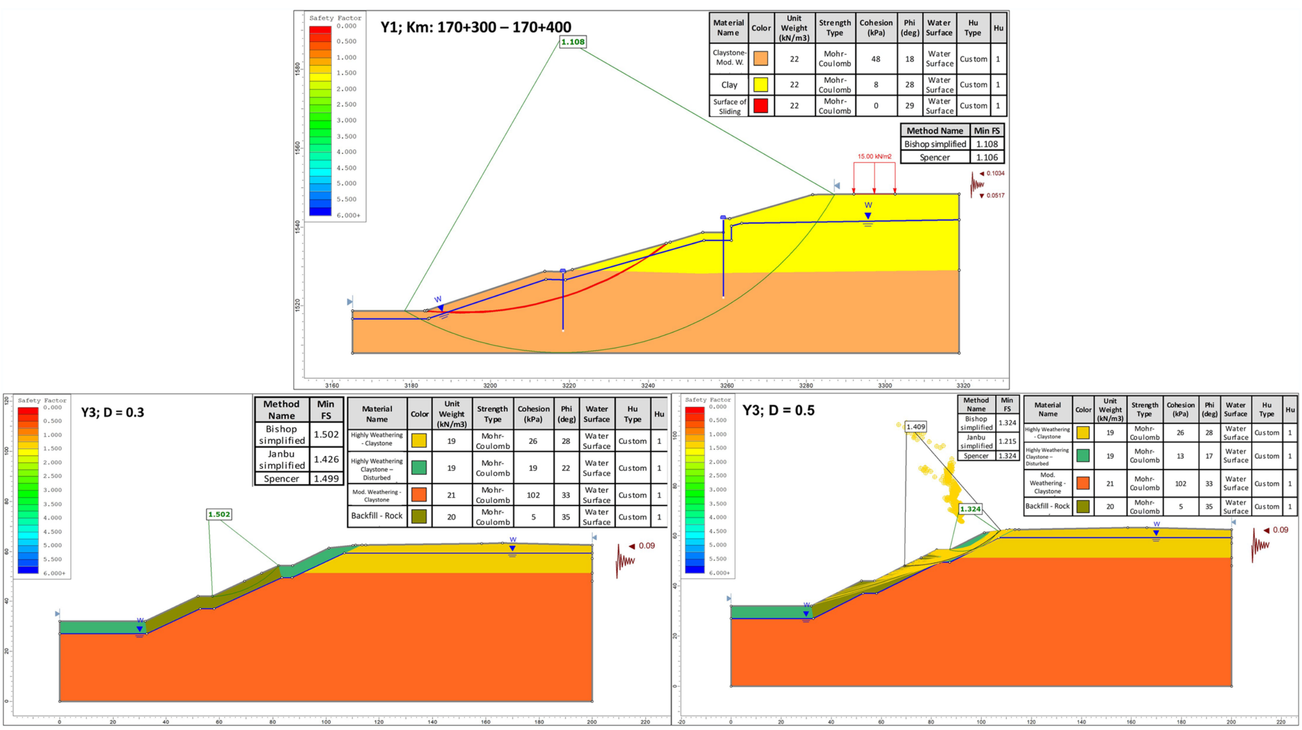

Fig. 18 Dynamic condition analysis of slope improvement in Y1 and Y3 mass movements

Evaluation of mass movement in km: 170 + 640 (Y2)

The translational slide in the Y2 cut slope occurred in February. According to the water budget, the months with the highest surface and groundwater in the region are December and March. In the field investigations made by the soil company, the slope angle of the critical discontinuity plane (β) was measured as 28° and the initial slope angle (α) was arranged to 27°. A mass movement developed at km: 170 + 640 on the slope. Upon evaluating the boreholes drilled in the region, along with the field observations and laboratory test results, it has been ascertained that the angle of internal friction angle (ϕ) value for the moderately weathered claystone, where a translational slide occurs, is 22° (in

Table 7 Map spectral acceleration coefficients (S_s and S_1), peak ground acceleration and velocity (PGA and PGV) and horizontal seismic coefficient (k_h) values of Y1 and Y3*

Mass Movement No	Local Soil Class	S_s	S_1	S_{DS}	S_{D1}	PGV	PGA (g)	PGA_{ground}	k_h
Y1	ZC	0.398	0.108	0.517	0.162	10.520	0.170	0.206	0.1034
Y3	ZC	0.359	0.104	0.467	0.156	9.853	0.156	0.187	0.0934

*$S_{s:}$ Short period map spectral acceleration coefficient for the period of 0.2 s, S_1: Short period map spectral acceleration coefficient for the period of 1.0 s, PGA: Peak Ground Acceleration, PGV: Peak Ground Velocity, S_{DS}: Short period design spectral acceleration coefficient, S_{D1}: Design spectral acceleration coefficient for 1.0 s

Table 8 Analysis results after slope improvements for Y1 and Y3 mass movements*

Mass Movement No	Slide 2- Factor of Safety Determination Method	Static State Long-Term (improved)		Requirement	Static State Long-Term (improved)		Requirement
Y1	Bishop Simplified	1.519		≥ 1.5	1.108		≥ 1.10
	Spencer	1.511			1.106		
Y3	Disturbance Factor (D)	$D = 0.3$	$D = 0.5$		$D = 0.3$	$D = 0.5$	
	Bishop Simplified	1.833	1.619		1.502	1.324	
	Janbu Simplified	1.747	1.491		1.426	1.215	
	Spencer	1.828	1.616		1.499	1.324	

*In addition to the solution proposed for slope improvements and the analysis results shown in Fig. 17 and Fig. 18, it is also suggested by the authors to construct a pile gravity wall project at the 2nd level of the bench to prevent damage to the dwelling located on the top of the slope in case of possible time-dependent development of a slip plane in the environment

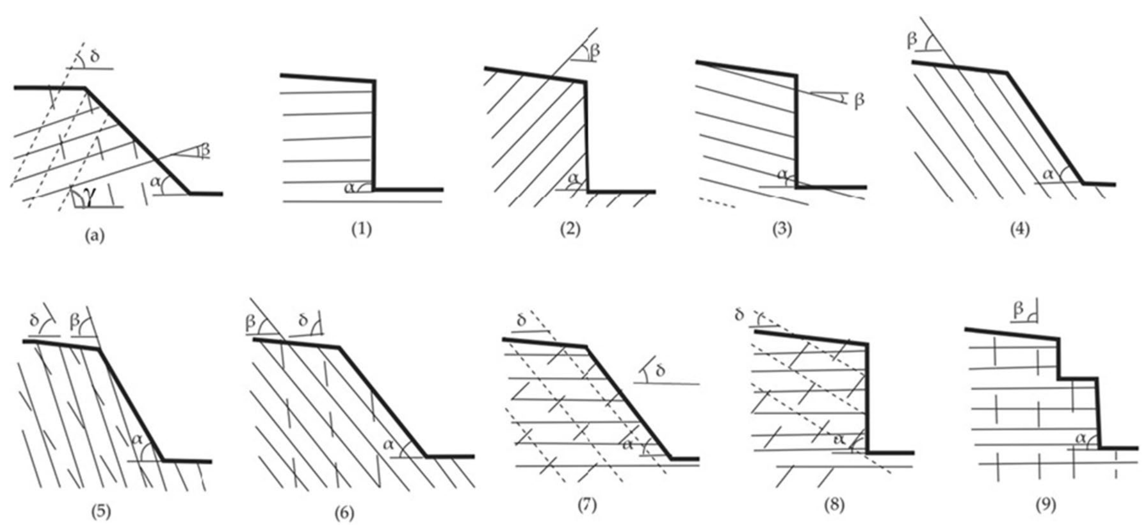

Fig. 19 Recommended appropriate slope angles to be arranged in the rocks according to the bed and fracture conditions (Erguvanlı 2016, modified from Terzaghi 1962)

conjunction with RMR and RocData software). Terzaghi (1962) suggested that the convenient slope angles should be given according to the fracture and layer conditions of the rocks empirically (Fig. 19). According to Fig. 19, the slope of Y2 (Fig. 9c) is an intense fractured rock mass as shown in case 4 in Fig. 19 ($\phi < \beta \rightarrow \alpha_c = \beta$). In this case, although the initial slope angle ($\alpha = 27°$) provides case number 4 shown in Fig. 19, it would be incorrect for the highly weathered fragmented fractured rock environment.

The gradient of the Y2 slope should be reduced to $\alpha \leq \phi$ to prevent the translational slide occurred in the Y2. Following the implementation of essential rehabilitation measures on the slope, it is advisable to conduct afforestation on the slope surface, ensure adequate drainage, and apply rip-rap protection to the slope surface.

Results and discussion

In the region where the Y1 mass movement occurs, it is proposed to construct a pile retaining wall for the first and second benches. It is aimed at ensuring the stability of the slope, stopping mass movements, and ensuring road safety by construction of these piles. As a result of the analyses made with Slide2 software using the limit equilibrium method, it has been suggested to design a retaining wall with 15 m long and 120 cm diameter piles on the first bench and 20 m long and 120 cm diameter piles on the second bench starting from the grade elevation to provide stability. The angle of the slope, designed as 22° before the landslide, was reduced to 17° with the proposed improvement techniques. The first and third cut slope ratio has been repositioned to be 3:1 (horizontal: vertical) and the second one is to be 3.5:1 (horizontal:vertical). In the static condition analysis performed after the improvement, the condition that the factor of safety value should be $FS \geq 1.5$ was sought. In the static condition analyses made because of the improvements, the factor of safety was found as $FS = 1.519$ with the Bishop Method and $FS = 1.511$ with the Spencer method. The factor of safety value should be $(FS) \geq 1.10$ when doing the slope analysis in dynamic conditions. In this study, this condition has been complied with in all dynamic condition analyses made because of the improvement. In the dynamic condition analyses made because of the improvements, the factor of safety was found as $FS = 1.108$ with the Bishop Method and $FS = 1.106$ with the Spencer method. No stability problems were encountered when the static and dynamic condition analyses of the designed pile retaining walls and the cut slope were performed.

In the Y2 cut with a maximum height of 40 m, in the area where the translational slide is observed, the shear force on the slip surface between vegetative soil on the upper and the moderately weathered claystone unit on the lower failed because of surface water and groundwater due to heavy rainfall, and the vegetal soil slid down throughout the slope under the control of gravity. The slope where the Y2 mass movement is located was excavated with an angle of 27°. The angle of the claystone layer was measured as $\beta = 28°$. The angle of internal friction was found as $\phi = 22°$ when the moderately weathered claystone unit, in which the Y2 translational slide took place, was evaluated with the RMR_{89} classification, Geological Strength Index (GSI) classification and RocData software. In the field, because of the field explorations, it was observed that the dip direction of the claystone layer and the dip direction of the slope were the same and the slope was arranged at the critical slope angle ($\alpha_c = 28°$). The recommended slope design angle for the gradient of the discontinuity causing sliding is primarily suggested to be equal to or less than the angle of internal friction. This adjustment aims to rehabilitate the Y2 translational sliding movement. Following the necessary slope adjustments, suggestions include implementing surface afforestation, artificial nature design, or applying rip-rap slope protection to enhance the stability of the sliding slope surface.

There is a ranch house on the upper part of the Y3 cut in which the flow-type movement occurred. As a result of the field observations, it was discovered that the walls of the dwelling collapsed while the Y3 cut was excavated, and cracks were formed in the pool of the dwelling due to the collapses that occurred because of the cut excavation. The activity was observed on the slope surface when the dwelling's pool water leaking from the cracks flowed. In the region where the Y3 mass movement is observed, there is a claystone unit belonging to the Ypresian Korucu Formation. Nevertheless, this unit shows different characteristics in terms of weathering within itself. There are two different units in the region highly weathered claystone and moderately weathered claystone. This situation caused the engineering geology parameters of the unit to be different. While performing stability analyses, a rotational slip-type mass movement that may develop over time on the slope was also taken into consideration. Analyses have been made in the association of three different weathering zones observed in the slope. The slope surface has first been evaluated as the undisturbed single claystone ($D = 0$) in accordance with the project design, and then analyses have been made for the disturbance factors $D = 0.3$ and $D = 0.5$. When stability analyses were performed with $D = 0.3$ disturbance, it was observed (Bishop $FS = 1.267$, Janbu $FS = 1.163$, Spencer $FS = 1.268$) that a landslide-type movement would not be expected in the region. Nevertheless, it has been observed that the long-term stability failed to provide the factor of safety values acquired. In the case of $D = 0.5$ disturbance, the obtained factor of safety values (Bishop $FS = 0.899$, Janbu $FS = 0.822$, Spencer $FS = 0.900$) has demonstrated that landslides could occur in the region even under static conditions.

Therefore, making stability improvement techniques in the region have been recommended. As a result of the analyses, it has been suggested to build rip-rap slope protection on the surface of the 1st and 2nd slopes to ensure stability. For the rip-rap slope protection proposed to be made on the slope surface, the properties of construction material are accepted as $c=5$ kPa, $\varphi=35°$, $\gamma=20$ kN/m^3. After the application of riprap to the 1st and 2nd slopes, the stability of the cut slope was evaluated in both dynamic and seismic conditions in this cut's improvement analysis, which has 3 benches and reaches 27 m in height. When the proposed rip-rap slope improvement is processed into Slide2 software, the factor of safety values for $D=0.3$ disturbance is FS = 1.833 with Bishop Method, FS = 1.747 with Janbu Method, FS = 1.828 with Spencer Method in the static condition, FS = 1.502 with Bishop Method, FS = 1.426 with Janbu Method and FS = 1.499 with Spencer Method in the dynamic condition. When the proposed rip-rap slope improvement is evaluated with $D=0.5$ disturbance in the Slide2 software, the factor of safety values for $D=0.5$ disturbance is FS = 1.619 with Bishop Method, FS = 1.491 with Janbu Method, FS = 1.616 with Spencer Method in the static condition, is FS = 1.324 with Bishop Method, FS = 1.215 with Janbu Method and FS = 1.324 with Spencer Method in the dynamic condition. When the static and dynamic analysis results with $D=0.3$ and $D=0.5$ disturbance are evaluated, it is seen that the increase in the weathering property of the rock has a ruinous effect on the stability. Designing a pile wall is suggested in this section to prevent any damage to the ranch house in case of possible sliding since units placed on the upper part of the area where mass movement occurred are unqualified and units situated in the transition zone are low strength parameters. As can be seen from the analysis, even if the water originating from the pool of the building is not in the environment, if no precautions are taken it is expected that the region will reach a $D=0.5$ disturbance value due to reasons such as excessive precipitation and continue the sliding movement observed in the first weathering situation. Therefore, even if there is no pool at the top of the cut, sliding-type movement will still be expected in the region. Although the proposed pile application was suggested after the flowing movement observed in the field, the region should be evaluated beforehand and the evaluations should be made accordingly, considering the geology of the environment and the presence of a structure at the top of the slope. Even if the proposed pile application was suggested after the flowing movement observed in the field, the region should be evaluated beforehand and the evaluations should be made accordingly, considering the geology of the environment and the presence of a structure at the top of the slope. In addition to this, structural measures should be taken to prevent movement and constructions such as a retaining wall should be applied for toe support on the field.

Conclusions

In the Kurtköy–Akyazı section of the Northern Marmara Motorway, within the 5th section, bounded by "the Motorway Port Connection Road" and "İzmit Junction", flow and slide type mass movements were observed along the route. The Y1, Y2, and Y3 slopes were evaluated within the scope of the engineering geology and geomechanical models. The causes of the mass movements and the applications for slope stabilization were evaluated. The project criteria prior to the occurrence of the mass movements were scrutinized for the static and dynamic cases, the types of mass movements, and the factors causing the mass movements were determined. The slope stabilization applications were included in the evaluations. Based on the field and laboratory test results of the mass movement zone formed in the right cut of the slope between 170 + 300–170 + 400 (Y1), 170 + 640 (Y2), and 175 + 297-175 + 463 (Y3) kilometers, the stability analyses were reconstructed by soil mechanical, engineering geological, and geotechnical evaluations.

The Y1 type of mass movement was defined as rotational landslide, the Y2 type of mass movement was defined as translational slide, and the Y3 type of mass movement was defined as flow during the field investigations. Mass movements were found to occur in the claystone–shale units of the Korucu Formation. The study area was analyzed for its hydrogeological characteristics. Accordingly, the Penman meteorological water balance was calculated in order to evaluate the study area in terms of understanding the evolution of the mechanism of mass movements with environmental characteristics and water conditions. According to the water balance, the surface and subsurface runoff in the study area is higher than normal. In the preparation of stability analyses, it was taken into account that the runoff is particularly intense in December and February and gradually decreases in the following months. When evaluating the geological structure of the study area, it was concluded that over time, due to weathering by water penetrating the claystone unit, the region turned into a residual soil under the influence of the groundwater table and surface water, causing mass movements.

The stability of the slopes is analyzed by calculating the cross sections within the limits of the beginning, the end of the slope and the mass movement, and the effect of the slope stability on the development of the mass movement. The stability of the cut slope was calculated for the slope head, and the parameters that negatively affect the stability were determined in the calculation section passing through the center of mass movement. In addition, engineering geological assessments of the large exposed area were evaluated with the data obtained from field and laboratory studies. The design parameters for the stability analysis for the cut slopes were determined and stability analyses were carried out. When the data obtained from the reclamation analyses were used in static and dynamic cases in the regions where mass movements occur, the designs were shown to be successful. During the study, it became clear once again that the deficiencies in the evaluation of engineering geology studies or study results in geotechnical projects cause additional costs for the project.

In summary, while this study has provided valuable insights into the causes of mass movements along the Kurtköy–Akyazı section named the 5th section of the Northern Marmara Motorway's, it is essential to acknowledge certain limitations and key findings. The limitations of this study include the inherent uncertainties associated with geological and geotechnical assessments, as well as the dynamic nature of environmental factors contributing to mass movements. In addition, the study focused on specific sections of the motorway, and extrapolation of the results to other regions should be done with caution. The effectiveness of proposed mitigation measures, such as pile retaining walls and embankment protection, may be influenced by site-specific conditions that were not fully captured in this study. Furthermore, the study emphasizes the importance of comprehensive geological analysis, but it is critical to recognize the evolving nature of geological processes and the potential for unforeseen challenges. Despite these limitations, the study emphasizes the importance of integrating engineering geology into geotechnical projects and highlights the success of the implemented design improvements in enhancing slope stability and mitigating the risks of mass movement along the Northern Marmara Motorway.

Acknowledgements The authors would like to thank Assoc. Prof. Dr. Ömer ÜNDÜL and Luke BUSHELL for their contribution to the study with their valuable recommendations, feedback and proofreading.

Author contributions M.Ç prepared the study from her master's thesis. M.Ç. wrote the manuscript under the supervision of E.B. and A.K. All authors M.Ç., E.B., and A.K. contributed to the final version of this manuscript. E.B. and A.K. supervised the master's thesis and the study.

Funding Open access funding provided by the Scientific and Technological Research Council of Türkiye (TÜBİTAK).

Data availability The data supporting the findings of this study are available in a public repository. Additional information regarding the data and materials used in this research is available from the corresponding author upon reasonable request.

Declarations

Competing interests The authors declare no competing interests.

References

AFAD (2019) Türkiye Earthquake Hazard Map. https://deprem.afad.gov.tr/deprem-tehlike-haritasi. Accessed 27 Aug 2020

Akkuş A (1995) Jeomorfolojiye Giriş, Öz Eğitim Yayınları, No: 2, Konya, (in Turkish)

Akkuş A (2007) Genel Fiziki Coğrafya, 2. Baskı, Nobel Yayın Dağıtım No: 71, Ankara, (in Turkish)

Aleotti P, Chowdhury R (1999) Landslide hazard assessment: Summary review and new perspectives. Bull Eng Geol Env 58:21. https://doi.org/10.1007/s100640050066.BerlinHeidelberg:Springer.ISSN1435-9529.OnlineISSN1435-9537

Altınlı, İ. E. (1968) Geological investigation of İzmit-Hereke-Kurucadağ area. MTA Bulletin; No: 71. (in Turkish)

Arslan A, Kelam MA, Eker AM, Akgun H, Koçkar MK (2014) Optical fiber technology to monitor slope movement. Engineering Geology for Society and Territory (eds. G. Lollino et al.), Vol. 2, pp. 1425–1429. https://doi.org/10.1007/978-3-319-09057-3_252

Arslan A, Akgün H, Koçkar MK, Eker AM, Kelam MA (2015) Fiber Optik Teknolojisi ile Heyelanların İzlenmesi. 3. Türkiye Deprem Mühendisliği ve Sismoloji Konferansı. İzmir, (in Turkish)

Arslan Kelam A, Koçkar MK, Akgun H (2016) Utilization of optical fiber system for mass movement monitoring. Disaster Sci Eng 2(1):19–24

Arslan Kelam A, Akgun H, Koçkar MK (2022) Application of an optical fiber-based system for mass movement monitoring. Environ Earth Sci 81:170. https://doi.org/10.1007/s12665-022-10289-w

Atterberg A (1911) Die Plastizita¨t der Tone. Internationale Mitteilungen Fuer Bodenkunde 1:10–43

Ayala I, Salinas C, Lopéz M, Espinoza J, Conde T, Salvidar S (2008) Inestabilidad de laderas. Mexico: CENAPRED, (in Spanish)

Ayala I (2000) Landslides: Landslides or ground movements? Definition, classifications, and terminology (p. 9). Mexico: Investigaciones Geográficas, UNAM, Bo

Babichev S, Kril TV, Shekhunova SB, Wójcik W (2021) Geo-Informational Approach to Risk Analysis of Slope Mass Movement. CITRisk'2021: 2nd International Workshop on Computational & Information Technologies for Risk-Informed Systems, September 16–17, Kherson, Ukraine. http://ceur-ws.org/Vol-3101/Short23.pdf

Baker VR (1958) Heyelanların Analizi, Karayolları Genel Müdürlüğü Yayınları No: 6, Ankara, (in Turkish)

Bates RL, Jackson JA (1987) Glossary of Geology. Falls Church, VA: American Geological Institute

Bieniawski ZT (1989) Engineering rock mass classifications: a complete manual for engineers and geologists in mining, civil, and petroleum engineering. John Wiley & Sons

Bieniawski ZT (1975) The Point Load Test in Geotechnical Practice (Cilt 9). Engineering Geology

Bishop AW (1955) The use of the slip circle in the stability analysis of earth slopes. Geotechnique (s. 7–17)

Budhu M (2011) Soil Mechanics and Foundations, 3rd edn. Wiley, New York, Pp, p 282

Çakıner M (2021) Kuzey Marmara Otoyolu Liman Bağlantı Yolu-İzmit Kavşağı Arası (5. Kesim) Kütle Hareketleri—Mekanik İyileştirme Uygulamaları. Dissertation, İstanbul, Maslak, Türkiye: İstanbul Technical University, (in Turkish)
Carter M, Bentley SP (1991) Correlations of soil properties. Pentech Press Publishers, London
Casagrande A (1932) Research on the atterberg limits of soil. Public Roads 13:121–136
Chen H, Lee CF (2004) Geohazards of slope mass movement and its prevention in Hong Kong. Eng Geol 76(1–2):3–25. https://doi.org/10.1016/j.enggeo.2004.06.003
Chiarle M, Geertsema M, Mortara G, Clague JJ (2021) Relations between climate change and mass movement: Perspectives from the Canadian Cordillera and the European Alps. Global Planet Change 202:103499. https://doi.org/10.1016/j.gloplacha.2021.103499
Claessens L, Temme AJAM, Schoorl JM (2013) Mass-movement causes: changes in slope angle. In: Shroder J. (Editor in Chief), Marston RA, Stoffel M (Eds.) Treatise on Geomorphology. Academic Press, San Diego, CA, vol. 7, Mountain and Hillslope Geomorphology, pp. 212–216. https://doi.org/10.1016/B978-0-12-374739-6.00167-6
Department of Scientific Documentation and Publicity (2016) Geoscience MapViewer and Drawing Editor http://yerbilimleri.mta.gov.tr/anasayfa.aspx. Accessed 27 Aug 2020
Eckel EB (1958) Landslides and Engineering Practice, By the Committee on Landslide Investigations, NAS-NRC Publication 544, Highway Research Board, Special Report 29. D. C, Washington, p 255
EPOCH (European Community Programme) (1993) Temporal Occurrence and Forecasting of Landslides in the European Community. In: Flageollet JC (Ed.), (Vol. 3), Contract no. 90 0025
Erguvanlı K (1995) Mühendislik Jeolojisi, 4. Baskı, Seç Yayın Dağıtım, İstanbul, (in Turkish)
Erguvanlı K (2016) Mühendislik Jeolojisi. Ankara: TMMOB Jeoloji Mühendisleri Odası, (in Turkish)
Erinç S (2010) Jeomorfoloji I, Güncelleştirilmiş 6. Baskı, Der Yayınları, No: 284, İstanbul, (in Turkish)
Ertunç A (2003) Mühendislik Jeolojisi, Süleyman Demirel Üniversitesi Yayınları No: 41, Isparta, (in Turkish)
Evans SG, Hungr O (1993) The assessment of rockfall hazards at the base of talus slopes, Canada. Canadian Geotech Journal 30:620–636
General Directorate of Highways (2013) Highways Technical Specifications. Türkiye, Ankara, (in Turkish)
Google Earth (2020) https://earth.google.com/web/. Accessed 1 August 2020
Guerra AJT, Fullen MA, Jorge MCO, Bezerra JFR, Shokr MS (2017) Slope processes, mass movement and soil erosion: a review. Pedosphere 27(1):27–41
Güney E (2004) Jeomorfoloji, Tekağaç Eylül Yayınları, Ankara, (in Turkish)
Güven IT (2022) Seismic vulnerability indices for ground in Derince-Kocaeli (NW Türkiye). Environ Earth Sci 81(5)
Hoek E (1994) Strength of rock and rock masses. ISRM News J 2(2):4–16
Hungr O, Leroueil S, Picarelli L (2013) Review, the Varnes classification of landslides types, an update. Landslides 11:67–194
Hutchinson J (1988) General report morphological and geotechnical parameters of landslides in relation to geology and hydrogeology. In; Bonnard C (Ed.), Proceedings (Vol. 1, pp. 3–35). Rotterdam, Netherlands: A. Balkema
Janbu N (1957) Earth pressure and bearing capacity by a generalized procedure of slices. Proceedings of the Fourth International Conference on Soil Mechanics, (s. 207–212). London, UK
Janbu N (1973) Slope Stability Computations. Hirschfield RC, Poulos SJ (eds.), Embankment-Dam Engineering, (s. 47–86). New York: John Wiley
Kaçka N (2019) Karamürsel (Kocaeli) Güneyi ve Güneybatısındaki Heyelanların Sismik Deformasyon Analizi. Doktora Tezi. Ankara: Ankara Üniversitesi Fen Bilimleri Enstitüsü, (in Turkish)
Karakaş A, Coruk Ö (2011) Impact of mass movements in the Kocaeli Province Turkey. Geol Today 27(2):70–73
Mesri G, Abdel-Ghaffar ME (1993) Cohesion Intercept in Effective Stress-Stability Analysis. Journal of Geotechnical Engineering
Micu M, Jurchescu M, Şandric I, Mărgărint MC, Chiţu Z, Micu D, Vasile, M (2016) Mass Movements. Landform Dynamics and Evolution in Romania, 765–820. https://doi.org/10.1007/978-3-319-32589-7_32
Ministry of Public Works and Settlement (2006) Disaster Regulation for Engineering Structures on Highway Route. Issue No: 26369. https://www.resmigazete.gov.tr/eskiler/2006/12/20061207-5.htm. Accessed 30 Aug 2020
Muchlis, Rakhman AN, Latifah U (2021) Analysis of land use for mitigating mass movement threats, case study: Wonolelo and its surrounding areas, Bantul Regency. In IOP Conference Series: Earth and Environmental Science (Vol. 871, No. 1, p. 012024). IOP Publishing. https://doi.org/10.1088/1755-1315/871/1/012024
Penman HL (1948) Natural evaporation from open water, bare soil, and grass. Proc Roy Soc Lond A 194:120–145
Rocscience Inc. (2004) RocData User's Guide, Strength analysis of rock and soil masses using the Generalized Hoek-Brown, Mohr-Coulomb, Barton-Bandis, and Power Curve failure criteria. Rocscience Inc.
Sadigov EN (2020) Simulation of mass movement during landslide processes in the agricultural landscape, Informatics and Control Problems 40 (2)
Sharpe CFS (1938) Landslides and Related Phenomena. Colombia University Press, New York
Shroder JF Jr, Bishop MP (1998) Mass movement in the Himalaya: new insights and research directions. Geomorphology 26(1–3):13–35
Skrzypczak I, Kokoszka W, Kogut J (2017) The Impact of Landslides on Local Infrastructure and the Environment. https://doi.org/10.3846/enviro.2017.049
Spencer E (1967) A method of analysis of the stability of embankments assuming parallel inter-slice forces. Geotechnique (s. 11–26)
Suárez J (1998) Deslizaminetos y estabilidad de taludes en zonas tropicales. Universidad Industrial de Santander, Bucaramanga, p. 540, (in Spanish)
Tang C, Tanyas H, Van Westen CJ, Tang C, Fan X, Jetten VG (2018) Analysing post-earthquake mass movement volume dynamics with multi-source DEMs. Eng Geol. https://doi.org/10.1016/j.enggeo.2018.11.010
Tarhan F (2002) Mühendislik Jeolojisi Prensipleri, Karadeniz Teknik Üniversitesi Yayınları, Trabzon, (in Turkish)
Tarı U (2007) İzmit Körfezi ve Çevresinin Morfotektoniği (Doktora Tezi). İstanbul Teknik Üniversitesi, Avrasya Yer Bilimleri Enstitüsü, İstanbul, (in Turkish)
TER (2018) Turkish Earthquake Regulation. Ministry of Interior, Disaster and Emergency Management Presidency. Ankara
Terzaghi K, Peck BR, Mesri G (1996) Soil Mechanics in Engineering Practice. John Wiley & Sons Inc
Terzaghi K (1950) Mechanism of landslides. The Geological Society of America: Application of Geology to Engineering Practice, Berken, Volume: pp.: 83–123
Terzaghi K (1962) Stability of Steep Slopes on Hard Unweathered Rocks. Geotechnique V:12, N:4, London
Timur E (2002) Üst Paleosen-Alt Eosen Kışlaköy formasyonu, Karabük-Safranbolu Tersiyer Havzası Güney Kenarı. Orta ve Doğu

Karadeniz Bölgesi'nin Litostratigrafi Adlamaları. (s. 12). M.T.A. Genel Müdürlüğü, (in Turkish)
Tiranti D, Cremonini R, Asprea I, Marco F (2016) Driving factors for torrential mass-movements occurrence in the western alps. Front Earth Sci 4:16. https://doi.org/10.3389/feart.2016.00016
Tokay M (1954) Kilyos Çayı Ağzı-Amasra-Bartın-Kozcağız-Çaycuma bölgesi jeolojisi hakkında rapor. Ankara: M.T.A, (in Turkish)
TTS Engineering (2018) Geotechnical Report of Port Connection Road - İzmit Junction (Section-5) on the Northern Marmara Motorway Project. Istanbul, (in Turkish)
Türkiye Earthquake Hazard Map Interactive Web Application (TEHMIWA) (2018) https://tdth.afad.gov.tr. Accessed 1 May 2021
Ulamış K, Kaçka N, Kılıç R (2017, November 9) Estimation of seismic slope displacements in North Anatolian Fault Zone, Karamürsel (Kocaeli, Türkiye). J African Earth Sci, 258–263. https://doi.org/10.1016/j.jafrearsci.2017.11.026
Ulusay R, Sönmez H (2006) Kaya Kütlelerinin Mühendislik Özellikleri. Ankara: T.M.M.O.B. Jeoloji Mühendisleri Odası Yayınları, (in Turkish)
Ünsal N (2006) İnşaat Mühendisleri İçin Jeoloji, Alp Yayınevi, Ankara, (in Turkish)
USGS (2004) Landslide Types and Process, E.U., The U.S. Geological Survey Landslide Program. Fact Sheet 2004–3072. US Department of Interior Geological Survey
Vallejo L, Ferrer M, Ortuño L, Oteo C (2002) Engineering Geology. Pearson Education, Madrid
Varnes DJ (1950) Relations of Landslides to Sedimentary Features, Applied Sedimentation, John Wiley, New York
Varnes DJ (1958) Landslide types and processes. Landslides and Engineering Practice, Special Report 29, E. B. Eckel, Ed., Highway Research Board, National Research Council, pp.: 20–47
Varnes DJ (1978) Slope Movement Types and Processes, Chapter 2 in Landslides: Analysis and Control, Special Report 176, R. L. Schuster, and R. J. Krizek, Eds., Highway Research Board, National Research Council
Wicander R, Monroe JS (2005) Fiziksel Jeoloji. (K. Dirik, & M. Şener) TMMOB Jeoloji Mühendisleri Odası Yayınları, (in Turkish)
Yağızel A, Özyavaş A (2020) İzmit Körfezinin Güneyindeki Kütle Hareketlerinin Kırık Sistemleri İle İlişkisinin ALOS PALSAR Verisi Kullanılarak İncelenmesi. Kocaeli Üniversitesi Fen Bilimleri Dergisi 3(1):77–89 ((**in Turkish**))
Zengince M, Karakaş, A (2018) Kocaeli Gölcük'te Oluşan Heyelanların Nedenleri, Etkileri ve Alınan Önlemler. Uygulamalı Yerbilimleri Dergisi, 17 (1), 39–54. https://doi.org/10.30706/uybd.418619, (in Turkish)
Zhou J, Li H, Lu G, Zhou Y, Zhang J, Fan G (2020) Initiation mechanism and quantitative mass movement analysis of the 2019 Shuicheng catastrophic landslide. Quarterly Journal of Engineering Geology and Hydrogeology, 54(2), qjegh2020–052. https://doi.org/10.1144/qjegh2020-052